

1 The ABCflux database: Arctic-Boreal CO₂ flux
2 observations and ancillary information aggregated to
3 monthly time steps across terrestrial ecosystems

4
5 Authors: Anna-Maria Virkkala¹, Susan M. Natali¹, Brendan M. Rogers¹, Jennifer D. Watts¹,
6 Kathleen Savage¹, Sara June Connon¹, Marguerite Mauritz², Edward A.G. Schuur³, Darcy Peter¹,
7 Christina Minions¹, Julia Nojeim¹, Roisin Commane⁴, Craig A. Emmerton⁵, Mathias Goeckede⁶,
8 Manuel Helbig^{7,8}, David Holl⁹, Hiroki Iwata¹⁰, Hideki Kobayashi¹¹, Pasi Kolari¹², Efrén López-
9 Blanco^{13,14}, Maija E. Marushchak^{15,16}, Mikhail Mastepanov^{14,17}, Lutz Merbold¹⁸, Frans-Jan W.
10 Parmentier^{19,20}, Matthias Peichl²¹, Torsten Sachs²², Oliver Sonnentag⁸, Masahito Ueyama²³,
11 Carolina Voigt^{15,8}, Mika Aurela²⁴, Julia Boike^{25,26}, Gerardo Celis²⁷, Namyi Chae²⁸, Torben R.
12 Christensen¹⁴, M. Syndonia Bret-Harte²⁹, Sigrid Dengel³⁰, Han Dolman³¹, Colin W. Edgar²⁹, Bo
13 Elberling³², Eugenie Euskirchen²⁹, Achim Grelle³³, Juha Hatakka²⁴, Elyn Humphreys³⁴, Järvi
14 Järveoja²¹, Ayumi Kotani³⁵, Lars Kutzbach⁹, Tuomas Laurila²⁴, Annalea Lohila^{24,12}, Ivan
15 Mammarella¹², Yojiro Matsuura³⁶, Gesa Meyer^{8,37}, Mats B. Nilsson²¹, Steven F. Oberbauer³⁸,
16 Sang-Jong Park³⁹, Roman Petrov⁴⁰, Anatoly S. Prokushkin⁴¹, Christopher Schulze^{8,42}, Vincent L.
17 St.Louis⁵, Eeva-Stiina Tuittila⁴³, Juha-Pekka Tuovinen²⁴, William Quinton⁴⁴, Andrej Varlagin⁴⁵,
18 Donatella Zona⁴⁶, Viacheslav I. Zyryanov⁴¹

19
20
21 1 Woodwell Climate Research Center, 149 Woods Hole Road Falmouth, MA, 02540-1644, USA
22 2 University of Texas, at El Paso, 500 W University Rd, El Paso, TX 79902, USA
23 3 Center for Ecosystem Science and Society, and Department of Biological Sciences, Northern
24 Arizona University, Flagstaff, AZ, 86001
25 4 Dept. of Earth & Environmental Sciences, Lamont-Doherty Earth Observatory, Columbia
26 University, Palisades, NY 10964
27 5 Department of Biological Sciences, University of Alberta, Edmonton, Alberta, Canada T6G
28 2E9
29 6 Dept. Biogeochemical Signals, Max Planck Institute for Biogeochemistry, Jena, Germany
30 7 Department of Physics and Atmospheric Science, Dalhousie University, Halifax, Nova Scotia,
31 Canada
32 8 Departement de Geographie, Universite de Montreal, Montreal, Quebec, Canada

33 9 Institute of Soil Science, Center for Earth System Research and Sustainability (CEN),
34 Universität Hamburg, Hamburg, Germany
35 10 Department of Environmental Science, Shinshu University, Matsumoto, Japan
36 11 Research Institute for Global Change, Japan Agency for Marine-Earth Science and
37 Technology, Yokohama, Japan
38 12 Institute for Atmospheric and Earth System Research/Physics, Faculty of Science, University
39 of Helsinki, Finland
40 13 Department of Environment and Minerals, Greenland Institute of Natural Resources, Kivioq
41 2, 3900, Nuuk, Greenland
42 14 Department of Bioscience, Arctic Research Center, Aarhus University, Frederiksborgvej 399,
43 4000 Roskilde, Denmark
44 15 Department of Environmental and Biological Sciences, University of Eastern Finland,
45 Kuopio, Finland
46 16 Department of Biological and Environmental Science, University of Jyväskylä, Jyväskylä,
47 Finland
48 17 Oulanka research station, University of Oulu, Liikasenvaarantie 134, 93900 Kuusamo,
49 Finland
50 18 Agroscope, Research Division Agroecology and Environment, Reckenholzstrasse 191, 8046
51 Zurich, Switzerland
52 19 Center for Biogeochemistry in the Anthropocene, Department of Geosciences, University of
53 Oslo, 0315 Oslo, Norway
54 20 Department of Physical Geography and Ecosystem Science, Lund University, 223 62 Lund,
55 Sweden
56 21 Department of Forest Ecology and Management, Swedish University of Agricultural
57 Sciences, 901 83 Umeå, Sweden
58 22 GFZ German Research Centre for Geosciences, Telegrafenberg, Potsdam, Germany
59 23 Graduate School of Life and Environmental Sciences, Osaka Prefecture University, 1-1
60 Gakuencho, Naka-ku, Sakai, 599-8531, Japan
61 24 Finnish Meteorological Institute, Climate system research, Helsinki, Finland
62 25 Alfred Wegener Institute Helmholtz Center for Polar and Marine Research, Telegrafenberg
63 A45, 14473 Potsdam, Germany & Geography Department, Humboldt-Universität zu Berlin,
64 Unter den Linden 6, 10099 Berlin, Germany
65 26 Geography Department, Humboldt-Universität zu Berlin, Berlin, Germany
66 27 Agronomy Department, University of Florida, Gainesville, USA
67 28 Institute of Life Science and Natural Resources, Korea University, 145 Anam-ro, Seongbuk-
68 gu, Seoul, 02841, Republic of Korea
69 29 Institute of Arctic Biology, University of Alaska Fairbanks, Fairbanks, AK 99775, USA
70 30 Earth and Environmental Sciences Area. Lawrence Berkeley National Lab, Berkeley, CA
71 94720, USA
72 31 Department of Earth Sciences, VU University of Amsterdam, Amsterdam, The Netherlands
73 32 Center for Permafrost, Department of Geosciences and Natural Resource Management,
74 University of Copenhagen, Øster Voldgade 10
75 33 Department of Ecology, Swedish University of Agricultural Sciences, Uppsala
76 34 Department of Geography & Environmental Studies, Carleton University, 1125 Colonel By
77 Dr. Ottawa, ON, K2B 5J5 Canada
78 35 Graduate School of Bioagricultural Sciences, Nagoya University, Nagoya, Japan

79 36 Forestry and Forest Products Research Institute
80 37 Environment and Climate Change Canada, Climate Research Division, Victoria, BC V8N
81 1V8, Canada
82 38 Department of Biological Sciences and Institute of Environment, Florida International
83 University, Miami Florida 33199 USA
84 39 Division of Atmospheric Sciences, Korea Polar Research Institute, 26 Songdomirae-ro
85 Yeonsu-gu, Incheon, Republic of Korea 21990
86 40 Institute for Biological Problems of Cryolithozone of the Siberian Branch of the RAS -
87 Division of Federal Research Centre “The Yakut Scientific Centre of the Siberian Branch of the
88 Russian Academy of Sciences
89 41 VN Sukachev Institute of forest SB RAS, Akademgorodok 50/28, Krasnoyarsk 660036
90 Russia
91 42 Department of Renewable Resources, University of Alberta, Edmonton, Alberta, Canada
92 T6G 2E9
93 43 School of Forest Sciences, University of Eastern Finland, Finland
94 44 Cold Regions Research Centre, Wilfrid Laurier University, Waterloo, Ontario, Canada, N2L
95 3C5
96 45 A.N. Severtsov Institute of Ecology and Evolution, Russian Academy of Sciences, 119071,
97 Leninsky pr.33, Moscow, Russia
98 46 Department of Biology, San Diego State University
99
100 ORCID iDs:
101 AMV: 0000-0003-4877-2918
102 SMN: 0000-0002-3010-2994
103 BMR: 0000-0001-6711-8466
104 MaM: 0000-0001-8733-9119
105 EAGS: 0000-0002-1096-2436
106 RC: 0000-0003-1373-1550
107 MG: 0000-0003-2833-8401
108 MH: 0000-0003-1996-8639
109 DH: 0000-0002-9269-7030
110 HI: 0000-0002-8962-8982
111 HK: 0000-0001-9319-0621
112 PK: 0000-0001-7271-633X
113 ELB: 0000-0002-3796-8408
114 MEM: 0000-0002-2308-5049
115 MiM: 0000-0002-5543-0302
116 LM: 0000-0003-4974-170X
117 FJP: 0000-0003-2952-7706
118 MP: 0000-0002-9940-5846
119 TS: 0000-0002-9959-4771
120 MU: 0000-0002-4000-4888
121 CV: 0000-0001-8589-1428
122 MA: 0000-0002-4046-7225
123 JB: 0000-0002-5875-2112
124 GC: 0000-0003-1265-4063

125 TRC: 0000-0002-4917-148X
126 MSB: 0000-0001-5151-3947
127 SD: 0000-0002-4774-9188
128 CE: 0000-0002-7026-8358
129 BE: 0000-0002-6023-885X
130 SEE: 0000-0002-0848-4295
131 AG: 0000-0003-3468-9419
132 EH: 0000-0002-5397-2802
133 JJ: 0000-0001-6317-660X
134 AK: 0000-0003-0350-0775
135 LK: /0000-0003-2631-2742
136 TL: 0000-0002-1967-0624
137 AL: 0000-0003-3541-672X
138 IM: 0000-0002-8516-3356
139 GM: 0000-0003-3199-5250
140 MBN: 0000-0003-3765-6399
141 SFO: 0000-0001-5404-1658
142 SJP: 0000-0002-6944-6962
143 RP: 0000-0002-6877-3902
144 ASP: 0000-0001-8721-2142
145 CS: 0000-0002-6579-0360
146 VLSiL: 0000-0001-5405-1522
147 EST: 0000-0001-8861-3167
148 JPT: 0000-0001-7857-036X
149 WQ: 0000-0001-5707-4519
150 DZ: 0000-0002-0003-4839
151 VIZ: 0000-0002-1748-4801
152 AV: 0000-0002-2549-5236
153 CAE: 0000-0001-9511-9191

154
155 Word count: 9200 (abstract: 302, main text: ~6900)
156 Corresponding author: Anna-Maria Virkkala, avirkkala@woodwellclimate.org
157

158

159

160

161

162 Abstract

163 Past efforts to synthesize and quantify the magnitude and change in carbon dioxide (CO₂) fluxes in
164 terrestrial ecosystems across the rapidly warming Arctic-Boreal Zone (ABZ) have provided valuable
165 information, but were limited in their geographical and temporal coverage. Furthermore, these efforts
166 have been based on data aggregated over varying time periods, often with only minimal site ancillary
167 data, thus limiting their potential to be used in large-scale carbon budget assessments. To bridge these
168 gaps, we developed a standardized monthly database of Arctic-Boreal CO₂ fluxes (ABCflux) that
169 aggregates *in-situ* measurements of terrestrial net ecosystem CO₂ exchange and its derived partitioned
170 component fluxes: gross primary productivity and ecosystem respiration. The data span from 1989 to
171 2020 with over 70 supporting variables that describe key site conditions (e.g., vegetation and disturbance
172 type), micrometeorological and environmental measurements (e.g., air and soil temperatures) and flux
173 measurement techniques. Here, we describe these variables, the spatial and temporal distribution of
174 observations, the main strengths and limitations of the database, and the potential research opportunities it
175 enables. In total, ABCflux includes 244 sites and 6309 monthly observations; 136 sites and 2217 monthly
176 observations represent tundra, and 108 sites and 4092 observations represent the boreal biome. The
177 database includes fluxes estimated with chamber (19 % of the monthly observations), snow diffusion (3
178 %) and eddy covariance (78 %) techniques. The largest number of observations were collected during the
179 climatological summer (June-August; 32 %), and fewer observations were available for autumn
180 (September-October; 25 %), winter (December-February; 18 %), and spring (March-May; 25 %).
181 ABCflux can be used in a wide array of empirical, remote sensing and modeling studies to improve
182 understanding of the regional and temporal variability in CO₂ fluxes, and to better estimate the terrestrial
183 ABZ CO₂ budget. ABCflux is openly and freely available online (Virkkala et al., 2021a).

184

185

186

187

188

189

190 1. Introduction

191

192 The Arctic-Boreal Zone (ABZ), comprising the northern tundra and boreal biomes, stores
193 approximately half the global soil organic carbon pool (Hugelius et al., 2014; Tarnocai et al.,
194 2009; Mishra et al., 2021). As indicated by this large carbon reservoir, the ABZ has acted as a
195 carbon sink over the past millenia due to the cold climate and slow decomposition rates (Siewert
196 et al., 2015; Hugelius et al., 2020; Gorham, 1991). However, these carbon stocks are increasingly
197 vulnerable to climate change, which is occurring rapidly across the ABZ (Box et al., 2019). As a
198 result, carbon is being lost from this reservoir to the atmosphere as carbon dioxide (CO₂) through
199 increased ecosystem respiration (Reco) (Schuur et al., 2015; Parker et al., 2015; Voigt et al.,
200 2017). The impact of increased CO₂ emissions on global warming depends on the extent to
201 which respiratory losses are offset by gross primary productivity (GPP), the vegetation uptake of
202 atmospheric CO₂ via photosynthesis (McGuire et al., 2016; Cahoon et al., 2016).

203

204 Carbon dioxide flux measurements provide a means to monitor the net CO₂ balance (i.e., net
205 ecosystem exchange; NEE, a balance between GPP and Reco) across time and space (Baldocchi,
206 2008; Pavelka et al., 2018). There are three main techniques used to measure fluxes at the
207 ecosystem level that represent fluxes from plants and soils to the atmosphere: eddy covariance,
208 automated and manual chambers, and snow diffusion methods (hereafter diffusion; for a
209 comparison of the techniques, see Table 1 in McGuire et al. 2012). The eddy covariance
210 technique estimates NEE at the ecosystem scale (ca. 0.01 to 1 km² footprint) at high temporal
211 resolution (i.e., ½ hr) using nondestructive and automated measurements (Pastorello et al., 2020).
212 Automated and manual chamber techniques measure NEE at fine spatial scales (< 1 m²) and in
213 small-statured ecosystems, common in the tundra, where the chambers can fit over the whole
214 plant community (Järveoja et al., 2018; López-Blanco et al., 2017). The diffusion technique, also
215 operating at fine spatial scales, can be used to measure the transport of CO₂ within a snowpack
216 (Björkman et al., 2010b). The eddy covariance technique has been used globally for over three
217 decades, and chamber and diffusion techniques for even longer.

218

219 Historically, the number and distribution of ABZ flux sites has been rather limited compared to
220 observations in temperate regions (Baldocchi et al., 2018). Due to these data gaps, quantifying

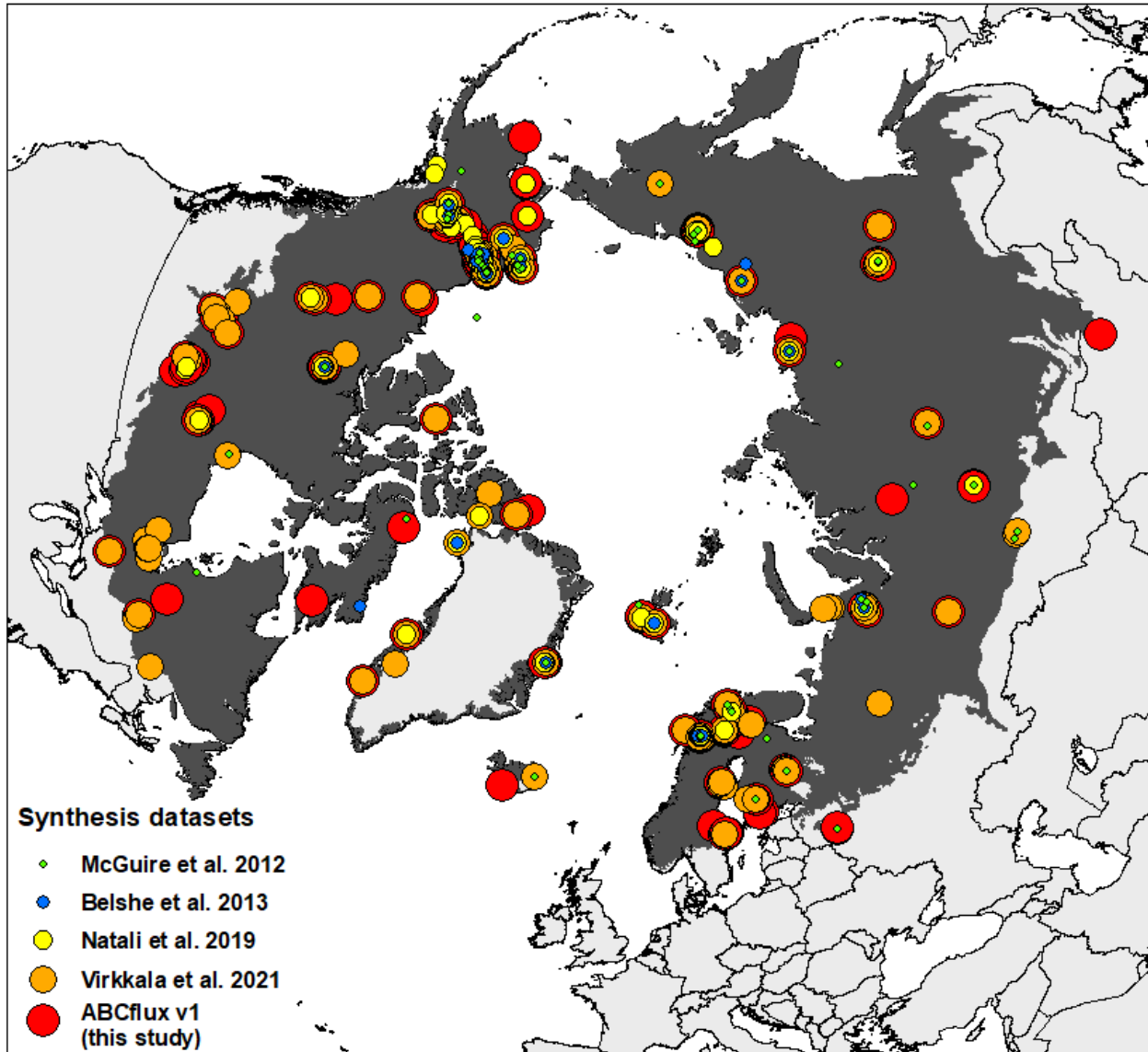
221 the net annual CO₂ balance across the ABZ has posed a significant challenge (Natali et al.,
222 2019a; McGuire et al., 2016; Virkkala et al., 2021). However, over the past decade, the
223 availability of ABZ flux data has increased substantially. Many, but not all, of the ABZ eddy
224 covariance sites are a part of broader networks, such as the global FLUXNET and regional
225 AmeriFlux, Integrated Carbon Observation System (ICOS) and the European Fluxes Database
226 Cluster (EuroFlux), where data are standardized and openly available (Paris et al., 2012; Novick
227 et al., 2018; Pastorello et al., 2020). These networks primarily include flux and meteorological
228 data, but do not often include other environmental descriptions such as soil carbon stocks,
229 dominant plant species, or the disturbance history of a given site (but see, for example,
230 Biological, Ancillary, Disturbance, and Metadata data in Ameriflux), which are important for
231 understanding the controls on CO₂ fluxes. Moreover, even though some ABZ annual chamber
232 measurements are included in the global soil respiration database (SRDB) (Jian et al., 2020), and
233 in the continuous soil respiration database (COSORE) (Bond-Lamberty et al., 2020),
234 standardized datasets providing ABZ CO₂ flux measurements from eddy covariance, chambers,
235 and diffusion, along with comprehensive metadata, have been nonexistent. Such an effort would
236 create potential for a more thorough understanding of ABZ CO₂ fluxes. Therefore, compiling
237 these flux measurements and their supporting ancillary data into one database is clearly needed
238 to support future modeling, remote sensing, and empirical data mining efforts.

239
240 Arctic-Boreal CO₂ fluxes have been previously synthesized in a handful of regional studies
241 (Belshe et al., 2013; McGuire et al., 2012; Luysaert et al., 2007; Baldocchi et al., 2018; Virkkala
242 et al., 2018; Natali et al., 2019a; Virkkala et al., 2021b) (Fig. 1 and Table 1). One of the main
243 challenges in these previous efforts, in addition to the limited geographical coverage of ABZ
244 sites and lack of environmental descriptions, has been the variability of the synthesized seasonal
245 measurement periods. Most of these efforts have allowed the seasonal definitions and
246 measurement periods to vary across the sites, creating uncertainty in the inter-site comparison of
247 flux measurements. An alternative approach to define seasonality is to focus on standard time
248 periods such as months (Natali et al., 2019a). Although focusing on monthly fluxes may result in
249 a small decrease in synthesizable data, because publications, particularly older ones, often
250 provide seasonal rather than monthly flux estimates (see e.g., (Euskirchen et al., 2012; Nykänen
251 et al., 2003; Björkman et al., 2010a; Oechel et al., 2000; Merbold et al., 2009)), compiling

252 monthly fluxes has several advantages over the seasonal fluxes. These advantages include: (i)
253 better comparability of measurements, (ii) ability to bypass problems related to defining seasons
254 across large regions, and (iii) ease of linking these fluxes to remote sensing and models.

255
256 Our goal is to build upon past synthesis efforts and compile a new database of Arctic-Boreal CO₂
257 fluxes (ABCflux version 1) that combines eddy covariance, chamber, and diffusion data at
258 monthly timescales with supporting environmental information to help facilitate large-scale
259 assessments of the ABZ carbon cycle. This paper provides a general description of the ABCflux
260 database by characterizing the data sources and database structure (Section 2), as well as
261 describing the characteristics of the database (Section 3). Additionally, we describe the main
262 strengths, limitations, and opportunities of this database (Section 4), and its potential utility for
263 future studies aiming to understand terrestrial ABZ CO₂ fluxes.

264



265

266 **Fig 1.** The flux site distribution in previous syntheses that focused on compiling fluxes from high
 267 latitudes (McGuire et al. 2012, Belshe et al. 2013, Natali et al. 2019a, Virkkala et al. 2021b and
 268 this study (ABCflux)). The Arctic-Boreal Zone is highlighted in dark grey; countries are shown
 269 in the background. Based on the unique latitude-longitude coordinate combinations in the tundra,
 270 there were 136 tundra sites in ABCflux, 104 tundra sites in Virkkala et al. 2021b, 68 tundra sites
 271 in Natali et al. 2019a, 34 tundra sites in Belshe et al. 2013, and 66 tundra sites in McGuire et al.,
 272 2012. Observations that were included in previous studies but not in ABCflux represent fluxes
 273 aggregated over seasonal, not monthly periods.

274

275 **Table 1.** A summary of past CO₂ flux synthesis efforts. If site numbers were not provided in the
 276 paper, this was calculated as the number of unique sets of coordinates.

Study	Number of sites	Synthesized fluxes and measurement techniques	Study domain	Study period	Flux aggregation
Luyssaert et al. (2007)	NA	GPP, Reco, and NEE measured with eddy covariance	Global forests (including boreal)	NA	Annual
McGuire et al. (2012)	66	GPP, Reco, and NEE measured with chambers, eddy covariance, diffusion technique and soda lime	Arctic tundra	Measurements from 1966-2009; focus on 1990-2009	Annual, growing and winter season
Belshe et al. (2013)	34	GPP, Reco, and NEE measured with chambers, eddy covariance, diffusion technique and soda lime	Arctic tundra	Measurements from 1966-2010	Annual, growing and winter season
Baldocchi et al. (2018)	9	GPP, Reco, and NEE measured with eddy covariance	Global (including boreal and tundra biomes)	NA (sites with 5-18 years of measurements)	Annual
Virkkala et al. (2018)	117	GPP, Reco, and NEE measured with chambers	Arctic tundra	Studies published during 2000-2016	Growing season
Natali et al. (2019a)	104	Soil respiration and NEE measured with chambers, eddy covariance, diffusion	Northern permafrost region	Measurements from 1989-2017, focus on 2000-2017	Monthly or seasonal during winter

		technique, and soda lime			
Virkkala et al. (2021b)	148	GPP, Reco, and NEE measured with chambers and eddy covariance	Arctic tundra and boreal biomes	1990-2015	Annual and growing season
ABCflux version 1 (this study)	244	GPP, Reco, and NEE (with some soil respiration and forest floor fluxes) measured with chambers, eddy covariance, and diffusion technique	Arctic tundra and boreal biomes	1989-2020	Monthly (whole year)

277

278 2. Data and methods

279 ABCflux focuses on the area covered by the northern tundra and boreal biomes (>45 °N), as
280 characterized in (Dinerstein et al., 2017), Fig. 2)), and compiles *in-situ* measured terrestrial
281 ecosystem-level CO₂ fluxes aggregated to monthly time periods (unit: g C m⁻² month⁻¹). We
282 chose this aggregation interval as monthly temporal frequency is a common, straightforward, and
283 standard interval used in many synthesis, modeling studies, remote sensing products, and process
284 model output (Didan, 2015; Natali et al., 2019a; Hayes et al., 2014). Furthermore, scientific
285 papers often report monthly fluxes, facilitating accurate extraction to ABCflux. We compiled
286 only aggregated fluxes to allow easy usage of the database, and to keep the database concise and
287 cohesive. We designed this database so that these monthly fluxes, compiled from scientific
288 papers or data repositories or contributed by site principal investigators (PIs), can be explored
289 from as many sites as possible and across different months, regions and ecosystems. The
290 database is not designed for studies exploring flux variability within a month, or how different
291 methodological decisions (e.g., flux filtering or partitioning approaches) influence the estimated
292 fluxes. If a potential data user requires fluxes at higher temporal frequency or is interested to

293 study the uncertainties related to flux processing, we suggest they utilize data from other flux
294 repositories (see Section 2.1.2.) or contact PIs.

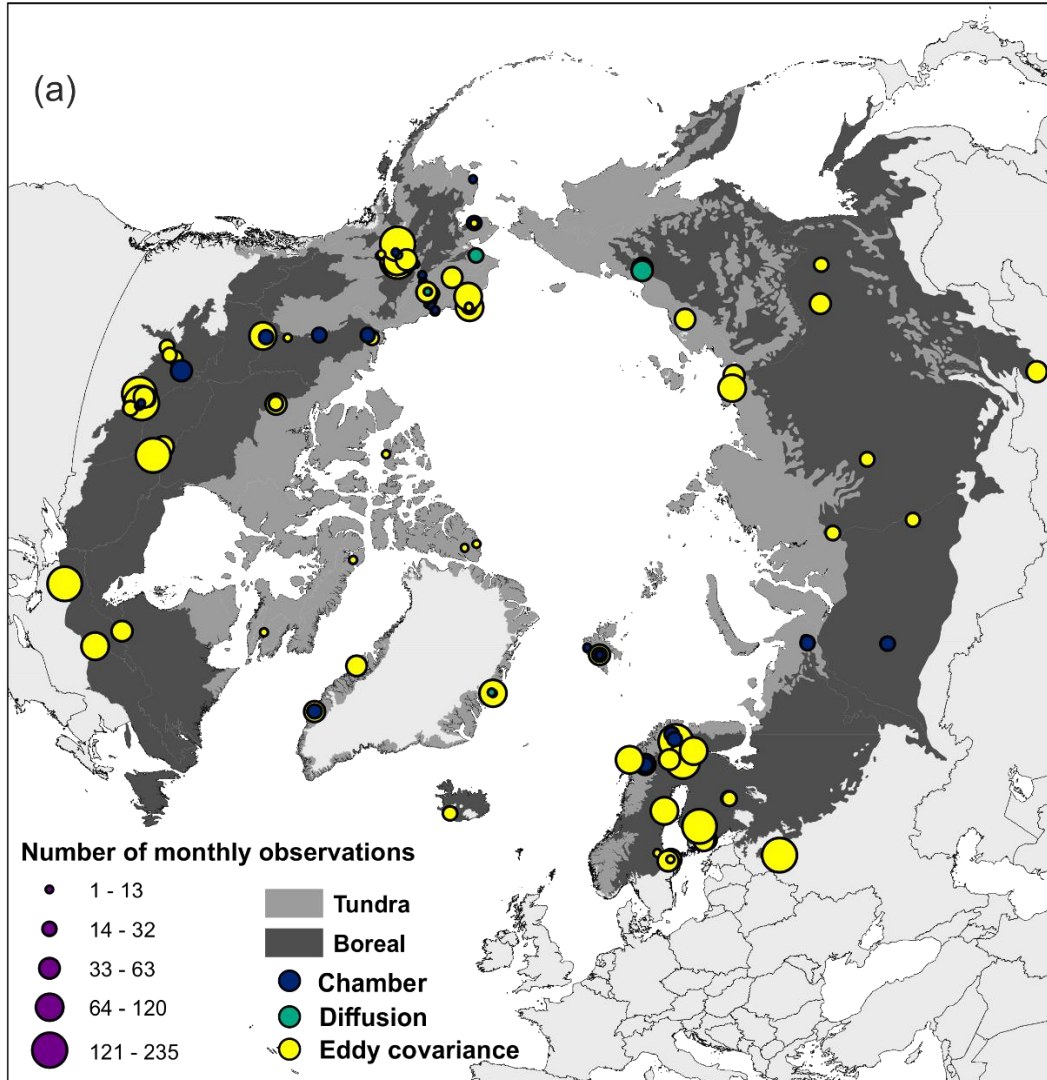
295

296 Although the three flux measurement techniques included in ABCflux primarily measure NEE,
297 chamber and eddy covariance techniques can also be used to estimate GPP (the photosynthetic
298 flux) and Reco (comprising emissions from autotrophic and heterotrophic respiration) (Keenan
299 and Williams, 2018), which are also included in the database. At eddy covariance sites, GPP and
300 Reco are indirectly derived from NEE using partitioning methods that primarily use light and
301 temperature data (Lasslop et al., 2010; Reichstein et al., 2005). At chamber sites, Reco can be
302 measured directly with dark chambers, from which GPP can be calculated by subtracting Reco
303 from NEE (Shaver et al., 2007). In general, these partitioned GPP and Reco fluxes have higher
304 uncertainties than the NEE measurements since they are modeled based on additional data and
305 various assumptions (Aubinet et al., 2012). However, GPP and Reco fluxes were included in
306 ABCflux because these component fluxes may help to better understand and quantify the
307 underlying processes of land–atmosphere CO₂ exchange.

308

309 In addition to CO₂ fluxes, we gathered information describing the general site conditions (e.g.,
310 site name, coordinates, vegetation type, disturbance history, a categorical soil moisture variable,
311 and soil organic carbon stocks), micrometeorological and environmental measurements (e.g., air
312 and soil temperatures, precipitation, soil moisture, snow depth), and flux measurement technique
313 (e.g., measurement frequency, instrumentation, gap-filling and partitioning method, number of
314 spatial replicates for chamber measurements, flux data quality), wherever possible.

315



317 **Fig 2.** Map showing the distribution and measurement technique at each site (a), and examples of
318 a manual chamber (b), diffusion measurements (c), and two eddy covariance towers in a
319 wetland-forest and tundra ecosystem (d-e). Photographs were taken in Kilpisjärvi, Finland (July
320 2016), Montmorency forest, Canada (April 2021), Scotty Creek, Canada (April, 2014), and
321 Yukon-Kuskokwim Delta, Alaska (September 2019). Image credits to: Markus Jylhä, Alex
322 Mavrovic, Gabriel Hould Gosselin, Chris Linder, Manuel Helbig.

323

324 2.1. Data sources

325 2.1.1 Literature search

326 We identified potential CO₂ flux studies and sites from prior synthesis efforts (Belshe et al.,
327 2013; McGuire et al., 2012; Virkkala et al., 2018; Natali et al., 2019a; Virkkala et al., 2021b),
328 including a search of citations within and of the studies included in these prior syntheses. We
329 also conducted a literature search with the search words (“carbon flux” or “carbon dioxide flux”
330 or “NEE” or “net ecosystem exchange”), and (“arctic” or “tundra” or “boreal”) in Web of
331 Science to ensure that our database included the most recent publications. We included studies
332 that reported at least NEE, presented at monthly or finer temporal resolution, and had supporting
333 environmental ancillary data describing the sites. We did not include fluxes reported at longer
334 timesteps (e.g., seasonal aggregations), which, based on our rough estimate, resulted in a 10-20
335 % loss of data from sites and periods that would have been new to ABCflux. These excluded
336 data primarily included some older, non-active eddy covariance sites and seasonal chamber
337 measurements (e.g., (Nobrega and Grogan, 2008; Heliasz et al., 2011; Fox et al., 2008)).
338 However, many of these data were located in the vicinity of existing sites covered by ABCflux
339 (e.g., Daring Lake, Abisko), thus excluding these measurements does not dramatically influence
340 the geographical coverage of the sites. We extracted our variables of interest (Section 2.3.) from
341 these selected papers during 2018-2020. Data from line and bar plots were extracted using Plot
342 Digitizer (<http://plotdigitizer.sourceforge.net/>) and converted to our flux units (g C m⁻² month⁻¹)
343 if needed. Data from experimental treatments were excluded; however, we included flux data
344 from unmanipulated control plots. Monthly non-growing season fluxes from Natali et al.,
345 (2019a) were extracted from the recently published data compilation (Natali et al., 2019b).

346 Winter chamber or diffusion measurements in forests from Natali et al., (2019b) were included in
347 the “ground_nee” field, which represents forest understory (not whole-ecosystem) NEE.

348

349 2.1.2. Flux repositories

350 We downloaded eddy covariance and supporting environmental data products from AmeriFlux
351 (Novick et al., 2018), Fluxnet2015 (Pastorello et al., 2020), EuroFlux database cluster (ICOS,
352 Carbon Extreme, Carbo Africa, GHG Europe, Carbo Italy, INGOS) (Paris et al., 2012; Valentini,
353 2003), and Station for Measuring Ecosystem-Atmosphere Relations (Hari et al., 2013). Data that
354 were filtered for USTAR (i.e., low friction velocity conditions) and gap-filled were downloaded
355 from repositories in 2018-2020. USTAR varied among sites due to differing site-level
356 assumptions. We downloaded only gap-filled data that met the USTAR criteria for either the
357 tower PI or given through the database processing pipeline. However, Fluxnet2015 provides
358 several different methods for determining data quality based on different USTAR criteria. In this
359 case, we used the Fluxnet2015 common USTAR threshold (CUT, i.e. all years at the site filtered
360 with the same USTAR threshold (Pastorello et al., 2020)). For observations extracted from
361 EuroFlux, USTAR thresholds for each site were derived as described in (Papale et al., 2006;
362 Reichstein et al., 2005) using night-time data. We extracted fluxes readily aggregated to monthly
363 intervals by the data processing pipeline from Fluxnet2015 and EuroFlux. These aggregations
364 were not given in AmeriFlux and SMEAR. We downloaded daily gap-filled data from these
365 repositories and summed the data to monthly time steps. We did not aggregate any repository
366 GPP, Reco, or NEE datasets that were not gap-filled. If fluxes were available for the same site
367 and period both in Natali et al., (2019b) and flux repository extractions, the flux repository
368 observations were kept in the database. Some repositories supplied eddy covariance data version
369 numbers, which were added to the flux database.

370

371 2.1.3. Permafrost Carbon Network data solicitation

372 A community call was solicited in 2018 through a CO₂ flux synthesis workshop (Parmentier et
373 al., 2019, Reconciling historical and contemporary trends in terrestrial carbon exchange of the
374 northern permafrost-zone, 2021), whereby the network of ABZ flux researchers were contacted

375 and invited to contribute their most current unpublished eddy covariance and chamber data. This
376 resulted in an additional 39 sites and 1372 monthly observations (see column extraction_source).
377

378 2.2. Partitioning approaches at eddy covariance flux sites

379 ABCflux compiles eddy covariance observations that were primarily partitioned using night-time
380 Reco, which is based on the assumption that during night, NEE measured at low light levels is
381 equivalent to Reco (Reichstein et al., 2005). This night-time partitioning approach has been the
382 most frequently used approach to fill gaps in flux time series (Wutzler et al., 2018) due to its
383 simplicity, strong evidence of temperature sensitivity of respiration, and direct use of Reco (i.e.
384 night-time NEE) flux data to estimate temperature response curves (Reichstein et al., 2005). As
385 the night-time approach was one of the first widely used partitioning approaches, fluxes
386 partitioned with the approach were the only ones available in the flux repositories at some of the
387 older sites. Daytime partitioning and other approaches started to develop more rapidly in the
388 2010s (Lasslop et al., 2010; Tramontana et al., 2020). Each of the partitioning approaches have
389 uncertainties related to the ecological assumptions, input data, model parameters, and statistical
390 approaches used to fill the gaps.

391
392 PIs that submitted data to us directly gap-filled and partitioned fluxes using the approach that
393 they determined works best at their site. Based on similar logic, fluxes extracted from papers
394 were not always partitioned using the night-time approach. In these cases, we trusted the
395 expertise of PIs and authors, and included fluxes partitioned using other methods. Although this
396 created some heterogeneity in the flux processing algorithms in the database, this approach was
397 chosen so that we could be more inclusive with the represented sites.

398
399 Thus, in summary, our goal was to compile fluxes that 1) can be easily compared with each other
400 (i.e., have been gap-filled and partitioned in a systematic way), 2) are as accurate as possible
401 given the site conditions and measurement setup (i.e., other approaches were accepted if this was
402 suggested by the PI), and 3) summarize information about the processing algorithms used.

403

404 2.3. Data quality screening

405 We screened for poor-quality data, potential unit and sign convention issues, and inaccurate
406 coordinates. Repository eddy covariance data were processed and quality checked using quality
407 flags associated with monthly data supplied by the repository processing pipeline. Fluxnet2015
408 and EuroFlux database include a data quality flag for the monthly aggregated data indicating
409 percentage of measured (quality flag QC = 0 in FLUXNET2015) and good-quality gap-filled
410 data (quality flag QC = 1 in FLUXNET2015; average from monthly data; 0=extensive gap-
411 filling, 1=low gap-filling); for more details see Fluxnet2015 web page
412 (<https://fluxnet.org/data/fluxnet2015-dataset/variables-quick-start-guide/>) and (Pastorello et al.,
413 2020)). Note that this quality flag field for the aggregated data differs from the ones calculated
414 for half-hourly data derived directly from eddy covariance tower processing programs (such as
415 Eddypro). We removed monthly data with a quality flag of 0. Data with quality flags >0 were
416 left within the database for the user to decide on additional screening criteria. Note that the
417 monthly data produced by the repository processing pipeline do not include separate gap-filled
418 percentages or errors of model fit for NEE similar to those associated with the half-hourly data.
419 However, we included these fields to the database as PIs contributing data or scientific papers
420 sometimes had this information; however these fields were not used in data quality screening.
421 Both the monthly quality flag and gap-filled percentage fields describe the amount and quality of
422 the gap-filled data that needed to be filled due to, for example, instrument malfunction, power
423 shortage, extreme weather events, and periods with insufficient turbulence conditions.

424

425 At chamber and diffusion sites, we disregarded observations including a low number of temporal
426 replicates within a month (<3 individual measurements in summer months) and only one
427 measurement month to ensure the temporal representativeness of the measurements. For the
428 spring (March-May), autumn (September-November), and winter (December-February) months,
429 one temporal replicate was accepted due to scarcity of measurements outside the summer season
430 (June-August); measurement frequency is included in the database. We excluded monthly
431 summertime measurements with <3 temporal replicates because within summer months,
432 meteorological conditions and the phenological status of the ecosystem can vary significantly
433 (Lafleur et al., 2012; Euskirchen et al., 2012; Schneider et al., 2012; Heiskanen et al., 2021), and
434 a single measurement is unlikely to capture this variability. Our decision to exclude

435 measurements that have only one measurement month was based on our goal to assess the
436 temporal variability of fluxes. We justified the acceptance of a lower number of temporal
437 replicates for the other seasons based on the assumption that flux variability is lower during the
438 winter months, and at least during most of the spring and autumn months, due to the insulating
439 effects of snow (Aurela et al., 2002; Bäckstrand et al., 2010). We estimate that excluding
440 measurements with <3 temporal replicates during the summer months resulted in a 10 % loss of
441 data. In total, 98 % of the chamber observations were from published studies; we assume that the
442 peer review process assessed the quality of published data.

443

444 We further screened for spatial coordinate accuracy by visualizing the sites on a map. If a given
445 site was located in water or had imprecise coordinates, the site researchers were contacted for
446 more precise coordinates. We screened for potential duplicate sites and observations that were
447 extracted from different data sources. Duplicate NEE extracted from papers that were also
448 extracted from flux repositories were compared to estimate uncertainties associated with paper
449 extractions using Plot Digitizer as a means for extracting monthly fluxes. A linear regression
450 between paper (Plot Digitizer) and repository extraction showed that data extracted using Plot
451 Digitizer were highly correlated with data from online databases, providing confidence in
452 estimates extracted using Plot Digitizer ($R^2=0.91$, slope = 1.002, $n=192$). Out of these duplicate
453 observations, we only kept the data extracted from the repository in the database. Finally, we
454 asked site PIs to verify that the resulting information was correct.

455

456 2.4. Database structure and columns

457 The resulting ABCflux database includes 94 variables: 16 are flux measurements and associated
458 metadata (e.g., NEE, measurement date and duration), 21 describe flux measurement methods
459 (e.g., measurement frequency, gap-filling method), 49 describe site conditions (e.g., soil
460 moisture, air temperature, vegetation type), and 8 describe the extraction source (e.g., primary
461 author or site PI, citation, data maturity). 61 variables are considered static and thus do not vary
462 with repeated measurements at a site (e.g., site name, coordinates, vegetation type), while 33
463 variables are considered dynamic and vary monthly (e.g., soil temperature). Table 2 includes a
464 description of each of the 94 variables, as well as the proportion of monthly observations present

465 in each column. ABCflux is shared as a comma separated values (csv) file with 6309 rows;
 466 however, not all the rows have data in each column (indicated by NA for character columns and -
 467 9999 for numeric columns).

468
 469 We refer to all fields included in ABCflux as “observations” although we acknowledge that, for
 470 example, GPP and Reco are indirectly derived variables at eddy covariance sites, and that some
 471 flux and ancillary data can also be partly gap-filled. Further, our database does not include the
 472 actual raw observations, rather it provides monthly aggregates. Positive values for NEE indicate
 473 net CO₂ loss to the atmosphere (i.e., CO₂ source) and negative numbers indicate net CO₂ uptake
 474 by the ecosystem (i.e., CO₂ sink). For consistency, GPP is presented as negative (uptake) values
 475 and Reco as positive.

477 **Table 2.** Database variables and the proportion of monthly observations in each variable. There
 478 are in total 6309 monthly observations in the database.

479

Variable	Variable description and units	Details	Proportion of monthly observations having data
id	ID given to each individual monthly entry at each site		100%
study_id	ID given to study/site entry (see Details)	(PI/first author of publication)_(site name)_(tower/chamber)_(#); Eg., Schuur_EML_Tower_1. Note that there might be several chamber (or tower) Study_IDs for one site.	100%
study_id_short	ID given to study/site entry (see Details), individual chamber plots within a site not differentiated	(PI/first author of publication)_(site name)_(tower/chamber)_(#); Eg., Schuur_EML_Tower_1.	100%
site_name	Site name as specified in data source	Usually the location name	100%

site_reference	A more specific name used in data source	For towers, this is often the acronym for the site, and for chambers, this is the name of the particular chamber plot	95%
country	Country of the site		100%
latitude	Decimal degrees, as precise as possible		100%
longitude	Decimal degrees, as precise as possible	Negative longitudes are west from Greenwich	100%
start_date	Date on which measurement starts	mm/dd/yyyy	100%
end_date	Date on which measurement ends	mm/dd/yyyy	100%
meas_year	Year in which data were recorded		100%
season	Season in which data were recorded	summer, autumn, winter, spring (based on climatological seasons)	100%
interval_month	Measurement month		100%
start_day	Start day of the measurement		100%
end_day	End day of the measurement		100%
duration	Number of days during the measurement month	Should be the same as End_Day because this database compiles monthly fluxes	100%

biome	Biome of the site	Boreal, Tundra	100%
veg_type	A detailed vegetation type for the site	B1=cryptogram, herb barren; B2=cryptogram barren complex; B3=noncarbonate mountain complex; B4=carbonatemountain complex; G1=rush/grass, forb, cryptogram tundra; G2=graminoid, prostrate dwarf-shrub, forb tundra; G3=nontussock sedge, dwarf-shrub, moss tundra; G4=tussock-sedge, dwarf-shrub, herb tundra; P1=prostrate dwarf-shrub, herb tundra; P2=prostrate/hemiprostrate dwarf-shrub tundra; S1=erect dwarf-shrub tundra; S2=low-shrub tundra; W1=sedge/grass, moss wetland; W2=sedge, moss, dwarf-shrub wetland; W3=sedge, moss, low-shrub wetland; DB=deciduous broadleaf forest; EN=evergreen needleleaf forest; DN=deciduous needleleaf forest; MF=mixed forest; SB=sparse boreal vegetation; BW=boreal wetland or peatland, following Watts et al. (2019). For more details about the tundra vegetation types, see Walker et al. (2005). These classes were classified based on information in Site_Reference and Veg_detail columns, or were contributed by the site PI.	100%
veg_type_short	A more general vegetation type for the site	B=barren tundra; G=graminoid tundra; P=prostrate dwarf-shrub tundra; S=shrub tundra; W=tundra wetland; DB=deciduous broadleaf forest; EN=evergreen needleleaf forest; DN=deciduous needleleaf forest; MF=mixed forest; SB=sparse boreal vegetation; BW=boreal wetland or peatland. For more details about the tundra vegetation types, see Walker et al. (2005). These classes were classified based on information in Site_Reference and Veg_detail columns, or were contributed by the site PI.	100%
veg_detail	Detailed vegetation description from data source/contributor		96%
permafrost	Reported presence or absence of permafrost	Yes, No	73%
disturbance	Last disturbance	Fire, Harvest, Thermokarst, Drainage, Grazing, Larval Outbreak, Drought	30%

disturb_year	Year of last disturbance	Numeric variable, 0 = annual (e.g., annual grazing)	23%
disturb_severity	Relative severity of disturbance	High, Low	11%
soil_moisture_class	General descriptor of site moisture	Wet = At least sometimes inundated or water table close to surface. Dry = well-drained.	56%
site_activity	Describes whether the site is currently active (i.e., measurements conducted each year)	Yes, No. Eddy covariance information was extracted from https://cosima.nceas.ucsb.edu/carbon-flux-sites/ by assuming that sites that were active in 2017 are still continuing to be active. We used our expertise to define active chamber sites that have measurements at least during each growing season.	60%
nee	Net Ecosystem Exchange (g C-CO ₂ m ⁻² for the entire measurement interval)	Convention: -ve is uptake, +ve is loss.	91%
gpp	Gross Primary Productivity (g C-CO ₂ m ⁻² for the entire measurement interval)	Report as -ve flux	68%
reco	Ecosystem Respiration (g C-CO ₂ m ⁻² for the entire measurement interval)	Report as +ve flux	73%
ground_nee	Forest floor Net Ecosystem Exchange, measured with chambers (g C-CO ₂ m ⁻² for the entire measurement interval)	Convention: -ve is uptake, +ve is loss. Chamber measurements from (primarily rather treeless) wetlands are included in the NEE_gC_m2 column.	4%
ground_gpp	Forest floor Ecosystem Respiration, measured with chambers (g C-CO ₂ m ⁻² for the entire measurement interval)	Report as -ve flux. Chamber measurements from (primarily rather treeless) wetlands are included in the GPP_gC_m2 column.	1%
ground_reco	Forest floor Gross Primary Productivity, measured with chambers (g C-CO ₂ m ⁻² for the entire measurement interval)	Report as +ve flux. Chamber measurements from (primarily rather treeless) wetlands are included in the Reco_gC_m2 column.	2%

rsoil	Soil respiration, measured with chambers (g C-CO ₂ m ⁻² for the entire measurement interval)	Report as +ve flux	4%
flux_method	How flux values were measured	EC=eddy covariance, Ch=chamber, Diff=diffusion methods. No observations from experimental manipulation plots	100%
flux_method_detail	Details related to how flux values were measured: closed- and open-path eddy covariance, mostly manual chamber measurements, mostly automated chamber measurements, a combination of chamber and cuvette measurements, diffusion measurements through the snowpack, chamber measurements on top of snow	EC_closed, EC_open, EC_enclosed, EC_open & closed, EC_enclosed, Chambers_mostly_manual, Chambers_mostly_automatic, Chambers_CUV, Snow_diffusion, Chambers_snow, NA	93%
measurement_frequency	Frequency of flux measurements	>100 characterizes high-frequency eddy covariance (and automated chamber) measurements. Manual chamber and diffusion techniques often have values between 1 and 30; 1=measurements done during one day of the month, 30=measurements done daily throughout the month. This is the primary variable that characterizes the frequency and gaps in monthly fluxes estimated with chambers and diffusion techniques.	100%
diurnal_coverage	Times of day covered by flux measurements	Day, Day and Night	90%
partition_method	Method used to partition NEE into GPP and Reco	Reichstein (night time=Reco partitioning), Lasslop (bulk/day-time partitioning), Reco_measured, ANN, or GPP=Reco-NEE (for chamber sites)	16%
spatial_reps_chamber	Number of spatial replicates for the chamber plot	Usually, but not always, several chamber plots are measured to assure the representativeness of measurements	71%
gap_fill	Gap filling method	e.g., Average, Linear interpolation, Lookup table, MDS (marginal distribution sampling), Light/temperature response, Neural network, a combination of these, or a longer description related to chamber measurements	70%

gap_perc	% of NEE data that was gap-filled in the measurement interval (relative to standard measurement time step)	Reported mainly for eddy covariance data	17%
tower_qa_qc_nee_flag	Overall monthly quality flag for eddy covariance aggregated observations; fraction between 0-1, indicating percentage of measured and good-quality gap-filled data	0=extensive gap-filling, 1=low gap-filling	44%
tower_qa_qc_nee_source	The source for the overall quality information for the eddy covariance observations	0=Fluxnet2015, 1=Euroflux	37%
method_error_nee	RMSE or other bootstrapped error of model fit for NEE (g C-CO ₂ m ⁻² for the entire measurement interval)		23%
method_error_technique	Technique used to quantify method errors for flux measurements	e.g., gap-filling and partitioning errors or uncertainty in data-model fit: bootstrap, MCMC, RMSE fit, etc.	1%
high_freq_availability	Availability of high-frequency data		17%
aggregation_method	Method used to aggregate data to measurement interval		58%
instrumentation	Description of instrumentation used		68%
tower_Version	Version number of the eddy covariance dataset from the extraction source		21%
tower_data_restriction			12%
tower_corrections	Details related to processing corrections employed, including time, duration, and thresholds		32%

	for u* and heat corrections		
spatial_variation_technique	Technique used to quantify spatial variation for flux measurements	e.g., standard error of replicate measurements for chambers, spatial error based on footprint partitioning for towers	10%
light_response_method_chamber	Details related to how the varying light response conditions were considered in chamber measurements		5%
par_cutoff	PAR level used to define nighttime data and apply partitioning method ($\mu\text{mol PAR m}^{-2} \text{ second}^{-1}$)		17%
precip_int	Total precipitation during measurement interval (mm)		37%
tair_int	Mean air temperature during measurement interval ($^{\circ}\text{C}$)		72%
tsoil	Mean soil Temperature during measurement interval ($^{\circ}\text{C}$)		74%
soil_moisture	Mean soil moisture during the measurement interval (% by volume)		35%
thaw_depth	Mean thaw depth during the measurement interval (cm)	Report with positive values	6%
tsoil_depth	Depth of soil temperature measurement below surface (cm)		46%
moisture_depth	Depth of soil moisture measurement below surface (cm)		31%
alt	Active layer thickness (cm; maximum thaw depth), will change annually	Report with positive values	15%

water_table_depth	Mean water table depth during the measurement interval (cm); Positive is below the surface, negative is above (inundated)		7%
snow_depth	Mean snow depth during the measurement interval (cm)		14%
vapor_pressure_deficit	Mean vapour pressure deficit during the measurement interval (Pa)		30%
evapotranspiration	Total evapotranspiration during the measurement interval (mm)		4%
par	Mean photosynthetically active radiation during measurement interval ($W\ m^{-2}$)		5%
par_ppfd	Mean photosynthetically active radiation during measurement interval (measured in Photosynthetic Photon Flux Density, PPFD; $\mu\text{mol}\ m^{-2}\ s^{-1}$)		11%
precip_ann	Mean annual precipitation (mm), from site or nearby weather station as a general site descriptor. This should describe the longer-term climate for the site rather than a few years of study.		80%
tair_ann	Mean annual air temperature ($^{\circ}C$), from site or nearby weather station as a general site descriptor. This should describe the longer-term climate for the site rather than a few years of study.		79%
t_precip_source_yrs	Data source and years used to calculate mean annual		50%

	temperature/precipitation		
elevation	Elevation above sea level (m)		65%
lai	Leaf Area Index		22%
sol_depth	Soil organic layer depth (cm)		23%
soil_perc_carbon	Soil carbon percentage (%)		7%
perc_C_depth	Depth at which soil carbon % was measured (cm)		7%
c_density	Soil carbon per unit area (kg C m ⁻²)		16%
c_density_depth	Depth to which soil organic carbon per unit area was estimated (cm)		8%
agb	Above ground biomass (kg C m ⁻²)		11%
agb_type	Types of above ground vegetation included in the AGB measurement	Trees, shrubs, graminoids, mosses, lichens	13%
soil_type	General soil type, including source (e.g., USDA, CSSC, NCSCD)		42%
soil_type_detail	Detailed soil type description, if available		9%
other_data	Other types of data from the data source that may be relevant		7%
notes_site_info	Any other relevant information related to static site descriptions		20%

notes_time_variant	Any other relevant information related to time-varying data		59%
citation	Journal article, data citation, and/or other source (online repository, PI submitted, etc.).		70%
citation_data_overlap	Another citation for the site		13%
data_contributor_or_author	Data contributor(s) or primary author(s) associated with data set or publication	If you use unpublished data or data from flux repositories (see Extraction_source), please contact this person	100%
email	Primary author email		93%
orcid	personal digital identifier: https://orcid.org/		29%
data_availability	Current availability of data: data available in a published paper, in an open online data repository, in an already published synthesis, or user contributed	Published_Paper, Published_Online, Published_Synthesis, User_Contributed	100%
data_maturity	Current maturity of data	Preliminary, Processed, Published, Reprocessed. Currently, none of the observations belong to the Preliminary or Reprocessed classes, but they were kept for future versions of the database.	100%
extraction_source	Data source	paper, Virkkala or Natali syntheses, Euroflux, Fluxnet 2015, PI, Ameriflux, SMEAR, ORNL DAAC, Pangea	100%
dataentry_person	The person(s) who added the data to the database	Primarily researchers working at Woodwell	100%

480

481

482

483 2.4. Database visualization

484 The visualizations in this paper were made with the full ABCflux database using each site-month
485 as a unique data point (from now on, these are referred to as monthly observations) and the sites
486 listed in the “study_id_short” field. We visualized these across the vegetation types

487 (“veg_type_short”), countries (“country”), biomes (“biome”), and measurement method
488 (“flux_method”).

489
490 To understand the distribution and representativeness of monthly observations and sites across
491 the ABCflux as well as the entire ABZ, we used geospatial data to calculate the aerial coverages
492 of each vegetation type and country. Vegetation type was derived from the European Space
493 Agency Climate Change Initiative’s (ESA CCI) land cover product aggregated and resampled to
494 0.0083° for the boreal biome (Lamarche et al., 2013) and the raster version of the Circumpolar
495 Arctic Vegetation Map (CAVM) for the tundra biome resampled to the same resolution as the
496 ESA CCI product (Raynolds et al., 2019). ESA CCI layers were reclassified by grouping land
497 cover types to the same vegetation type classes represented by ABCflux: boreal wetland and
498 peatland (from now on, boreal wetland; classes 160, 170, 180 in ESA CCI product), deciduous
499 broadleaf forest (60-62), evergreen needleleaf forest (70-72), deciduous needleleaf forest (80-
500 82), mixed forest (90), and sparse and mosaic boreal vegetation (40, 100, 100, 120, 121, 122,
501 130, 140, 150, 151, 152, 153, 200, 201, 202). Croplands (10, 11, 12, 20, 30) and urban areas
502 (190) were removed. We used the five main physiognomic classes from CAVM in the tundra.
503 Glaciers and permanent water bodies included in either of these products were removed. Note
504 that in ABCflux and for the site-level visualizations in this paper, vegetation type for each of the
505 flux sites was derived from site-level information, not these geospatial layers. These same
506 glacier, water, and cropland masks were applied to the country boundaries (Natural Earth - Free
507 vector and raster map data at 1:10m, 1:50m, and 1:110m scales, 2021) to calculate the terrestrial
508 area of each country. We further used TerraClimate annual and seasonal air temperature and
509 precipitation layers averaged over 1989-2020 to visualize the distribution of monthly
510 observations across the Arctic-Boreal climate space (Abatzoglou et al., 2018).

511

512 3. Database summary

513 3.1. General characteristics of the database

514 ABCflux includes 244 sites and 6309 monthly observations, out of which 136 sites and 2217
515 monthly observations are located in the tundra (54 % of sites and 52 % of observations from

516 North America, 46 % and 48 % from Eurasia), while 108 sites and 4092 monthly observations
 517 are located in the boreal biome (59 % of sites and 58 % of observations from North America, 41
 518 % and 42 % from Eurasia) (Table 3). The largest source of flux data are the flux repositories (48
 519 % of the monthly observations), while flux data extracted from papers or contributed by site PIs
 520 amount to 30 % and 22 % of the monthly observations, respectively. The database primarily
 521 includes sites in unmanaged ecosystems, but it does contain a small number (6) of sites in
 522 managed forests.

523

524 **Table 3.** General statistics of the database. Number of monthly CO₂ flux measurements and sites
 525 derived from eddy covariance, chamber, and diffusion techniques, and the proportion of data
 526 coming from different data sources. Note that some of the data extracted from flux repositories
 527 and papers were further edited by the PIs; this information can be found in the database. For this
 528 table, observations that were fully contributed by the PI were considered as PI-contributed.

529

Flux measurement technique	Number of sites	Number of monthly observations	Number of monthly observations derived using different eddy covariance and chamber techniques	Number of monthly observations extracted from different data sources
Eddy covariance	Total: 119 Tundra: 47 Boreal: 72	Total: 4957 Tundra: 1406 Boreal: 3551	Open-path: 1988 Closed path: 2085 Both: 245 Enclosed: 240 No information available: 399	Flux repository: 2775 Published: 810 PI-contributed: 1350
Chamber	Total: 104 Tundra: 73 Boreal: 31	Total: 1166 Tundra: 708 Boreal: 458	Manual: 435 Automated: 696 No information available: 35	Flux repository: 243 Published: 901 PI-contributed: 22
Diffusion	Total: 21 Tundra: 16 Boreal: 5	Total: 186 Tundra: 103 Boreal: 83		Flux repository: 0 Published: 186 PI-contributed: 0

530

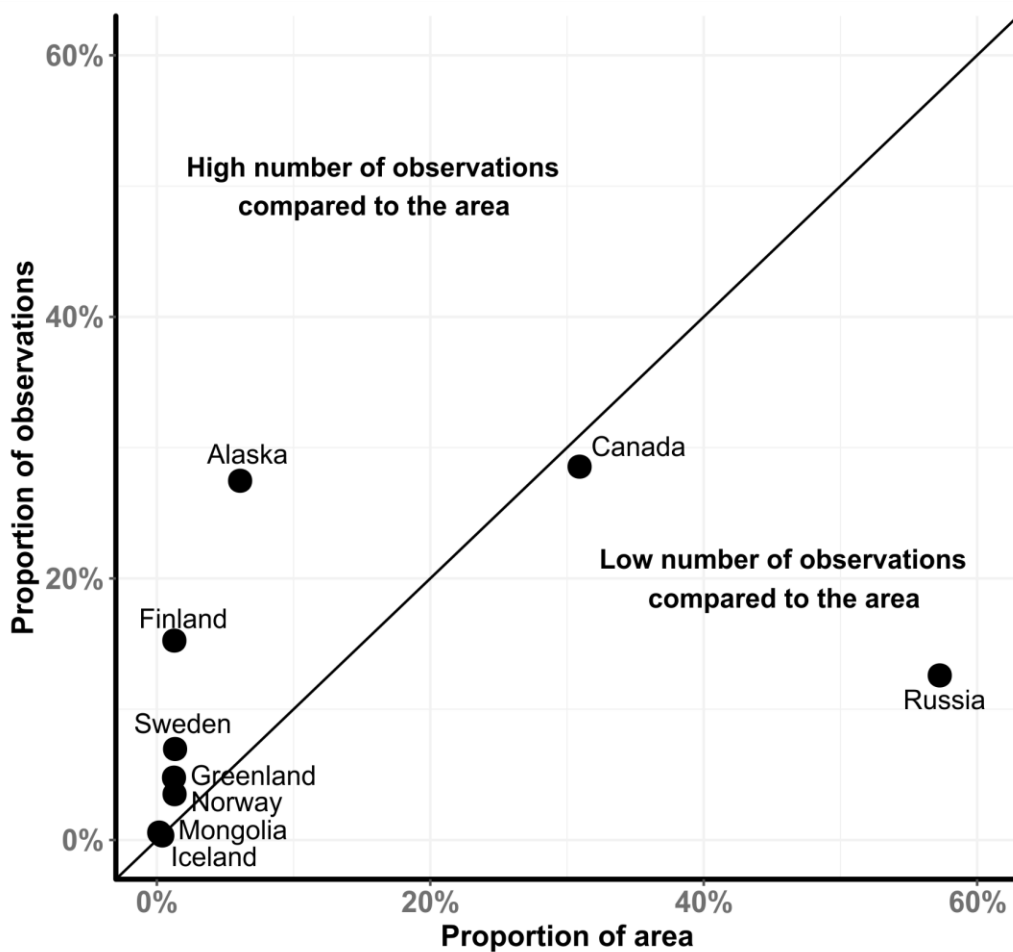
531

532 The majority of observations in ABCflux have been measured with the eddy covariance
533 technique (119 sites and 4957 monthly observations), whereas chambers and diffusion methods
534 were used at 125 sites and 1352 observations (Table 3). About 46 % of the eddy covariance
535 measurements are based on gas analyzers using closed-path technology (including enclosed
536 analyzers), 40 % are based on open-path technology, 5 % include both and 8 % are unknown. 52
537 % of chamber measurements were automated chambers (monitoring the fluxes continuously
538 throughout the growing season). Only 3 % of the measurements were completed using diffusion
539 methods during the winter. Chamber and diffusion studies were primarily from the tundra and
540 the sparsely treed boreal wetlands, but a few studies with ground surface CO₂ fluxes from forests
541 (i.e., capturing the ground cover vegetation and not the whole ecosystem) are also included in
542 their own fields so that they can not be mixed up with ecosystem-scale measurements
543 (“ground_nee”, ”ground_gpp”, “ground_reco”). Further, a few soil CO₂ flux sites measuring
544 fluxes primarily on unvegetated surfaces during the non-growing season are included in the
545 database (“rsoil”). These were included in the database because ground surface or soil fluxes
546 during the non-growing season can be of similar magnitude to the ecosystem-level fluxes when
547 trees remain dormant (Ryan et al., 1997; Hermle et al., 2010). Therefore, these ground or soil
548 fluxes could potentially be used to represent ecosystem-level fluxes during some of the non-
549 growing season months. However, we did not make an extensive literature search for these
550 observations, rather we compiled observations if they came up in our NEE search. Therefore, the
551 data in these ground surface and soil flux columns represents only a portion of such available
552 data across the ABZ.

553
554 The geographical coverage of the flux data is highly variable across the ABZ, with most of the
555 sites and monthly observations coming from Alaska (37 % of the sites and 28 % of the monthly
556 observations), Canada (19 % and 29 %), Finland (7 % and 15 %), and Russia (14 % and 13 %)
557 (Fig. 3). The sites cover a broad range of vegetation types, but were most frequently measured in
558 evergreen needleleaf forests (23 % of the sites and 37 % of the monthly observations) and
559 wetlands in the tundra or boreal zone (30 % and 27 %) (Fig. 4). The northernmost and
560 southernmost ecosystems had fewer sites and observations than more central ecosystems (barren
561 tundra: 45% of the sites and 3 % of the monthly observations, prostrate shrub: 2 % and <1 %,
562 deciduous broadleaf forest: 1 % and 3 %, deciduous needleleaf forest: 5 % and 4 %, mixed forest

563 <1 % and <1 %). The sites in ABCflux cover the most frequent climatic conditions across the
564 Arctic-Boreal zone relatively well; however, conditions with high precipitation and low
565 temperatures are lacking sites (Fig. 5). ABCflux includes sites experiencing various types of
566 disturbances, with the majority of disturbed sites encountering fires (24 sites and 901 monthly
567 observations), thermokarst (4 sites and 113 monthly observations), or harvesting (6 sites and 258
568 monthly observations). However, ABCflux is dominated by sites in relatively undisturbed
569 environments or sites lacking disturbance information (only 20 % of the sites and 30 % of the
570 monthly observations include disturbance information).

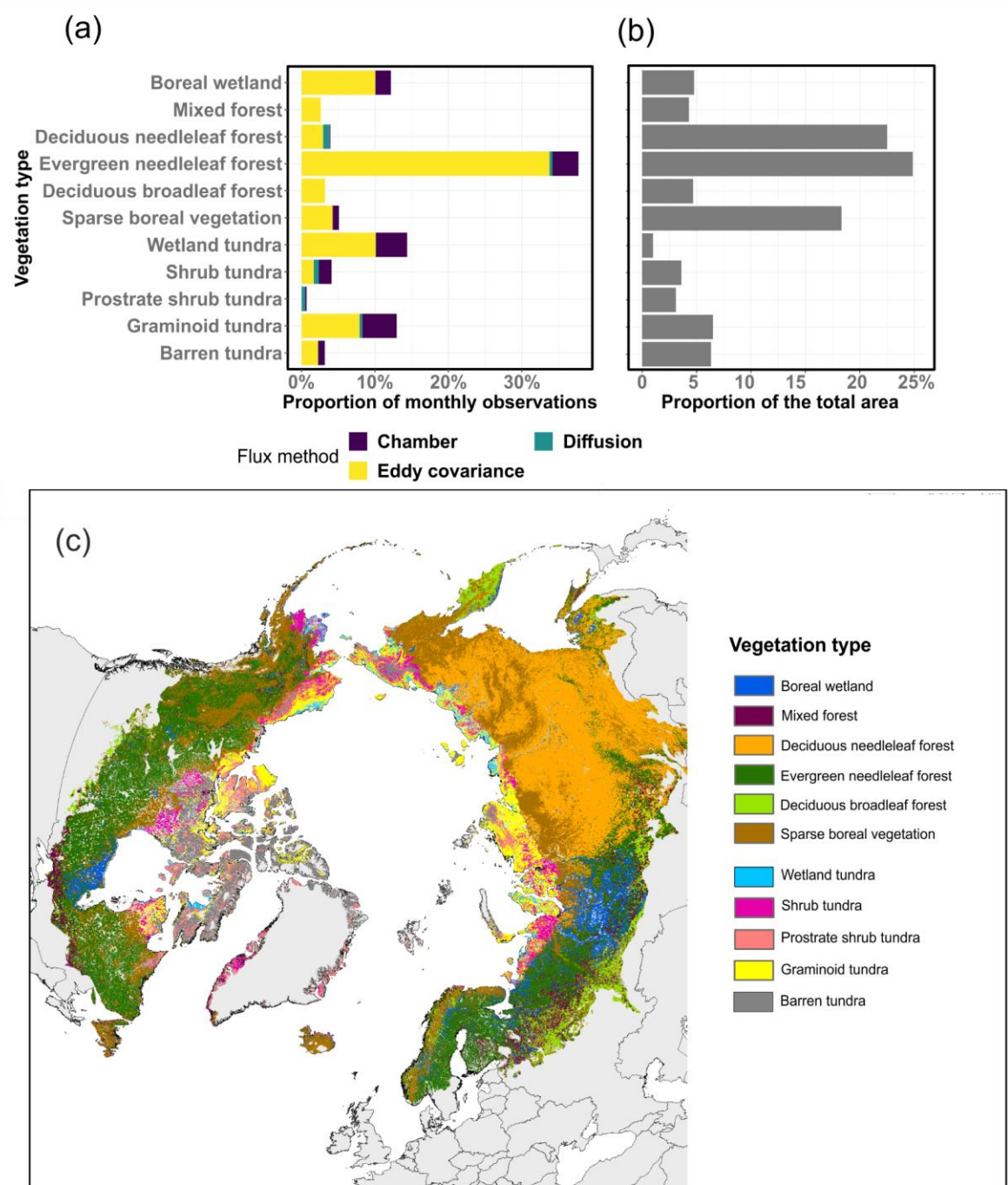
571



572

573 **Fig 3.** The proportion of monthly observations in each country/region compared to the
 574 proportion of the areal extent of the country/region across the entire Arctic-Boreal Zone. Ideally,
 575 points would be close to the 1:1 line (i.e., large countries/regions have more observations than
 576 small countries/regions). Permanent water bodies, glaciers, croplands, and urban areas were
 577 masked from the areal extent calculation.

578



579

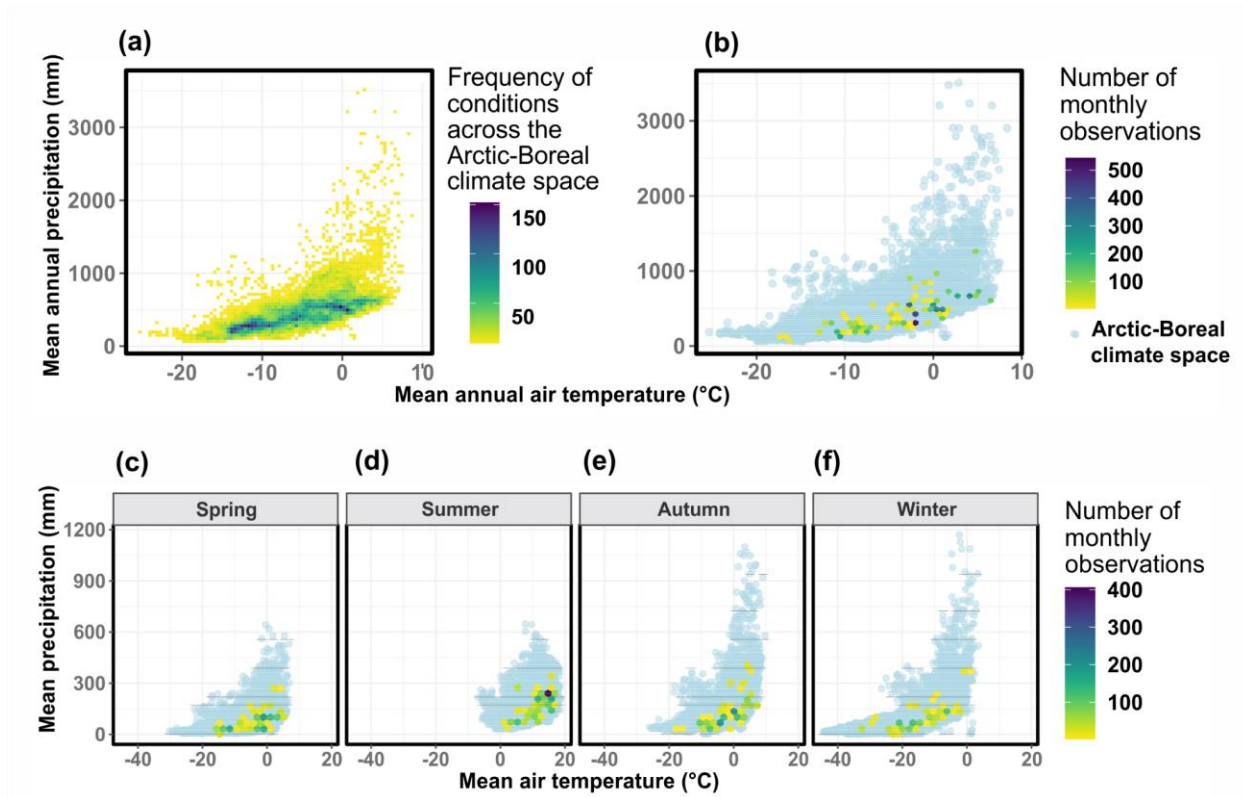
580

581 **Fig 4.** The proportion of monthly observations in each vegetation type colored by the flux
582 measurement technique (a) and the proportion of the areal extent of each vegetation type across
583 the entire Arctic-Boreal Zone (b). Permanent water bodies, croplands, and urban areas were
584 masked from the areal extent calculation. Sparse boreal vegetation class in the vegetation map
585 includes vegetation mixtures and mosaics.

586

587 ABCflux spans a total of 31 years (1989-2020), but the largest number of monthly observations
588 originate from 2000-2015 (80 % of the data) (Fig. 6). The reason for a decrease in flux data over
589 2015-2020 is likely related to a reporting lag, not a decrease in flux sites and records. The largest
590 number of measurements were conducted during the summer (June-August; 32 %) and the least
591 during the winter (November-February; 18 %) (Fig. 5 and 6). The overall eddy covariance data
592 quality and gap-filled data percentage were lowest during the winter compared to other seasons
593 (0.76 compared to 0.8-0.85 for overall data quality, 0=extensive gap-filling, 1=low gap-filling;
594 69 % compared to 47 to 59 % for gap-filled data percentage).

595



596

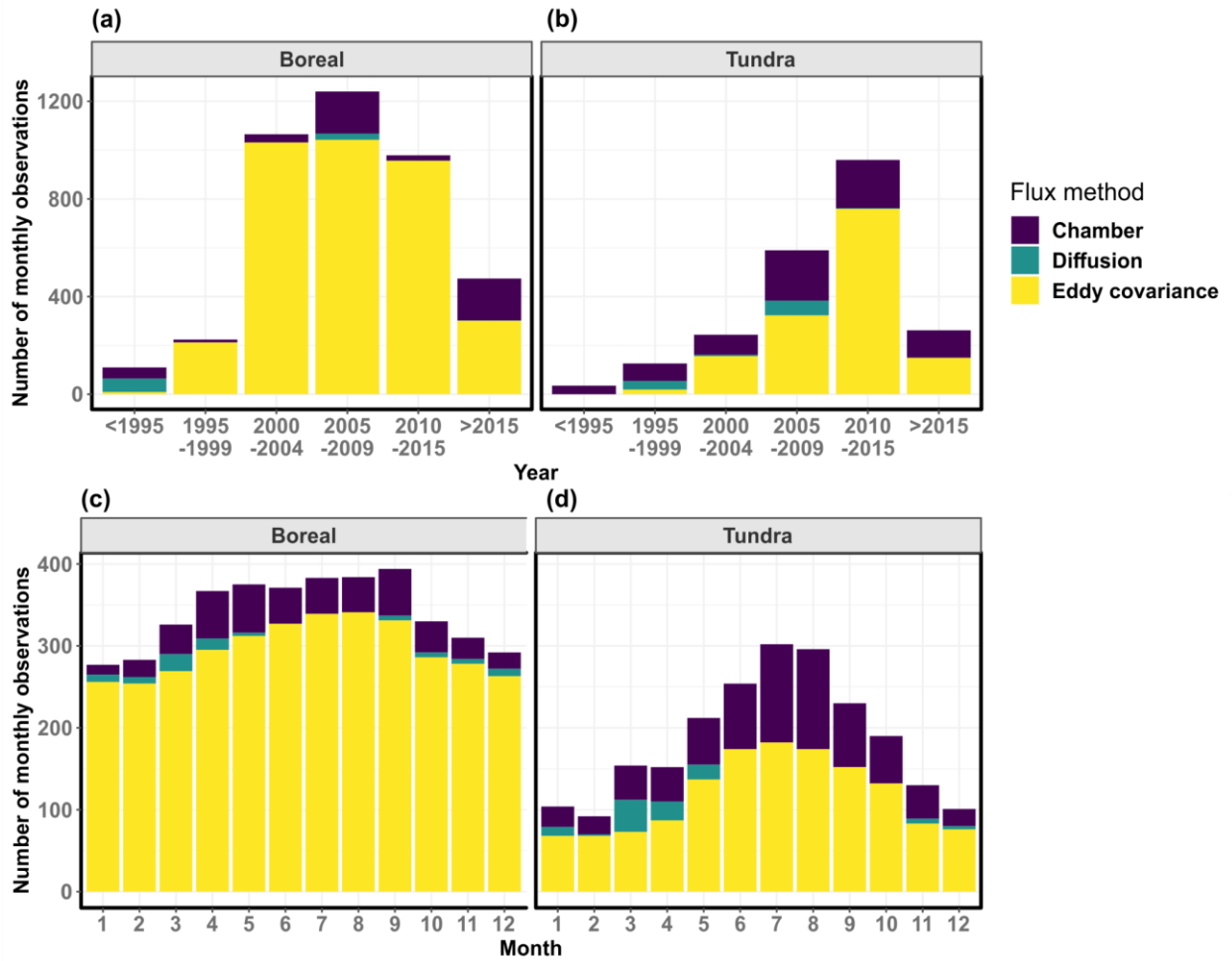
597 **Fig 5.** Mean annual air temperature and precipitation conditions across the Arctic-Boreal zone

598 (a), the entire ABCflux (b), and the air temperature and precipitation conditions across the

599 different climatological seasons included in ABCflux (c-f). Arctic-Boreal climate space was

600 defined based on a random sample of 20000 pixels across the domain.

601



602

603 **Fig 6.** Histograms showing the number of monthly measurements across five-year periods (a-b)

604 and across months (c-d) across the tundra and boreal biomes. The bar plots are colored by the

605 flux measurement technique. Chambers in the boreal biome measured fluxes in treeless or

606 sparsely treed areas (primarily wetlands).

607

608 3.2. Coverage of ancillary data

609

610 All of the observations in ABCflux include information describing the site name, location,

611 vegetation type, NEE, measurement technique (eddy covariance/chamber/diffusion), and how the

612 data were compiled (Table 2). Details about the measurement technique (e.g., open or closed-

613 path eddy covariance, manual or automated chambers) are included in 93 % of sites and 93 % of

614 monthly observations. Most of the monthly observations further include information about

615 permafrost extent (67 % of the sites and 72 % of the monthly observations), or soil moisture
616 state (47 % of the sites and 56 % of the monthly observations). Data describing air temperature,
617 soil temperature, precipitation, and soil moisture are included in 71, 73, 37, and 35 % of monthly
618 observations, respectively. Some ancillary variables have low data coverage, such as soil organic
619 carbon stocks (16 % of the monthly observations) or active layer thickness (15 % of the monthly
620 observations).

621

622 3.3. Coverage and distribution of flux data

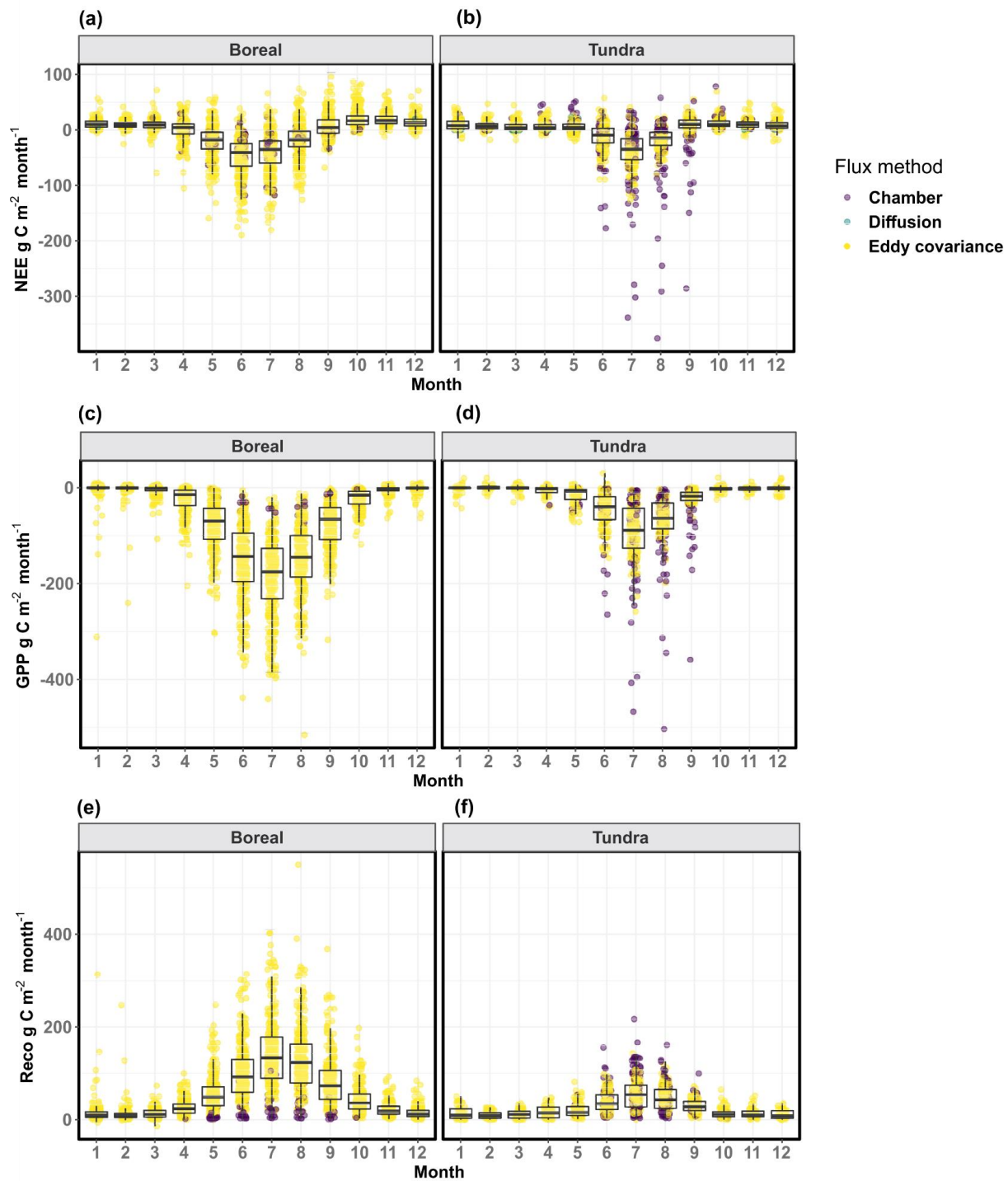
623

624 There are 110 sites and 4290 monthly observations for GPP, 121 sites and 4603 monthly
625 observations for Reco, and 212 sites and 5759 monthly observations for NEE in ABCflux.
626 Monthly values range from -2 to -516 g C m⁻² month⁻¹ for GPP, from 0 to 550 g C m⁻² month⁻¹
627 for Reco, and from -376 to 95 g C m⁻² month⁻¹ for NEE (Table 4). NEE is typically negative
628 during the summer (i.e., net CO₂ sink) and mostly positive during other seasons (i.e., net CO₂
629 source) (Fig.7). Out of all site and year combinations, annual cumulative NEE (the sum of
630 monthly NEE values for each year and site) can be calculated for 267 site-years. An average
631 annual NEE calculated based on the site-level averages from 1995 to 2020 is -27.9 g C m⁻² year⁻¹
632 (SD 85.4) for the entire region, -35.5 g C m⁻² year⁻¹ (SD 93.7) for the boreal biome, and -3.3 g C
633 m⁻² year⁻¹ (SD 44.2) for the tundra. However, these averages do not account for the spatial or
634 temporal distribution of the observations, and therefore represent coarse summaries of the
635 database.

636

637

638



639
 640 **Fig 7.** The distribution of net ecosystem exchange (NEE; a-b), gross primary productivity (GPP;
 641 c-d), and ecosystem respiration (Reco; e-f) across the months and biomes, colored by the flux
 642 measurement technique. Positive numbers for NEE indicate net CO₂ loss to the atmosphere (i.e.,
 643 CO₂ source) and negative numbers indicate net CO₂ uptake by the ecosystem (i.e., CO₂ sink).

644 For consistency, GPP is presented as negative values and Reco as positive. The boxes correspond
 645 to the 25th and 75th percentiles. The lines denote the 1.5 IQR of the lower and higher quartile,
 646 where IQR is the inter-quartile range, or distance between the first and third quartiles. There is
 647 not much chamber data from the boreal regions as they capture NEE only at treeless wetlands.
 648

649 **Table 4.** Mean and standard deviation of monthly observations of net ecosystem exchange
 650 (NEE), gross primary productivity (GPP), and ecosystem respiration (Reco) in $\text{g C m}^{-2} \text{ month}^{-1}$.
 651 Seasons were defined based on the climatological definition (autumn: September-November;
 652 winter: December-February; spring: March-May; summer: June-August). Positive numbers for
 653 NEE indicate net CO_2 loss to the atmosphere (i.e., CO_2 source) and negative numbers indicate
 654 net CO_2 uptake by the ecosystem (i.e., CO_2 sink). For consistency, GPP is presented as negative
 655 values and Reco as positive. Some sites compute only NEE and, consequently, NEE summaries
 656 might not entirely match with GPP and Reco statistics.

657
 658
 659

Biome	Climatological season	Mean monthly NEE (standard deviation)	Mean monthly GPP (standard deviation)	Mean monthly Reco (standard deviation)
Boreal	spring	-5 (25)	-40 (49)	34 (32)
Boreal	summer	-35 (36)	-163 (79)	124 (71)
Boreal	autumn	14 (18)	-38 (45)	52 (46)
Boreal	winter	11 (8)	-3 (19)	14 (20)
Tundra	spring	6 (9)	-11 (16)	18 (14)

Tundra	summer	-26 (38)	-72 (60)	48 (30)
Tundra	autumn	10 (21)	-14 (30)	21 (15)
Tundra	winter	9 (10)	-2 (9)	12 (11)

660 4. Strengths, limitations, and opportunities

661 ABCflux provides several opportunities for an improved understanding of the ABZ carbon cycle.
662 It can be used to calculate both short- and longer-term monthly, seasonal, or annual flux
663 summaries for different regions, or it can be combined with remote sensing and other gridded
664 data sets to build monthly statistical and process-based models for CO₂ flux upscaling. ABCflux
665 can further be utilized to study the inter- and intra-annual CO₂ flux variability resulting from
666 climate and environmental change. The site distribution in ABCflux can also be used to evaluate
667 the extent of the current flux network and identify under-sampled regions. From a
668 methodological perspective, data users can compare fluxes estimated with the different
669 measurement techniques which can help understand the uncertainties associated with individual
670 techniques. However, there are also some uncertainties that the data user should be aware of
671 when using ABCflux, which we describe below.

672

673 4.1. Comparing fluxes estimated with different techniques

674 The ABCflux database comprises aggregated observations using eddy covariance, chamber, and
675 diffusion methods. These methods measure CO₂ fluxes at different spatiotemporal resolutions
676 and are based on different assumptions. The eddy covariance technique is currently the primary
677 method to monitor long-term trends in ecosystem CO₂ fluxes (Baldocchi et al., 2018; Baldocchi,
678 2008), and the majority of observations in ABCflux (79 %) have been made using the technique.
679 Transforming high-frequency eddy covariance measurements to budgets includes several
680 processing steps that can, without harmonization and standardization of these steps (Baldocchi et
681 al., 2001; Pastorello et al., 2020), lead to highly different budget estimates (Soloway et al.,
682 2017). It is also important to acknowledge that the extent and size of the tower footprint differs
683 across the sites due to differences in the height of the tower and the direction and magnitude of

684 the wind (Chu et al., 2021). When fluxes are aggregated over longer time periods to cumulative
685 budgets, one generally assumes the tower footprint remains relatively constant, capturing fluxes
686 from a similar part of the ecosystem (i.e., the assumption that monthly observations within one
687 site in ABCflux can be reliably compared with each other); but note that at shorter time periods
688 this might not be the case (Pirk et al., 2017; Chu et al., 2021).

689

690 The different gas analyzer technologies also play an important role for the fluxes estimated with
691 the eddy covariance technique. Sites located in the most northern and remote parts of the ABZ
692 experience a drop in irradiation during autumn and winter which limits solar power availability
693 for eddy covariance measurements. Closed-path systems require more power to run than open-
694 path sensors, but open-path sensors are known to have larger uncertainties. For example, open-
695 path eddy covariance sensors have been shown to incorrectly estimate NEE due to the self-
696 heating effect of the analyzer, which can result in systematically higher net CO₂ uptake
697 compared to closed-path sensors (Kittler et al., 2017a); however, this pattern was not clearly
698 observed in ABCflux when across-site comparisons were made. Furthermore, wintertime fluxes
699 indicating CO₂ uptake can be erroneous due to the limited ability of the gas analyzer to resolve
700 very high frequency turbulent eddies (Jentsch et al., 2021). Recently, some types of open-path
701 infrared gas analysers have been found to be prone to biases in NEE that scale with sensible heat
702 fluxes in all seasons rather than with self-heating (Wang et al., 2017; Helbig et al., 2016).

703

704 While using eddy covariance to estimate small-scale spatial variability in NEE is challenging
705 (McGuire et al., 2012), this can be accomplished with chamber and diffusion techniques.
706 Chamber measurements can be done in highly heterogeneous environments as long as chamber
707 closure can be guaranteed; however, most of the chamber measurements in ABCflux have been
708 conducted in relatively flat and homogeneous graminoid- and wetland-dominated vegetation
709 types. Most chamber sites in ABCflux include ca.10-20 individual plots in total from ca. 3-5 land
710 cover types where fluxes are being measured (Virkkala et al., 2018). Chambers can also provide
711 more direct estimates of Reco and GPP relative to eddy covariance-derived fluxes, and are
712 therefore useful for estimating the magnitude and range of those component fluxes. However,
713 manual chamber and diffusion measurements are laborious and have limited temporal
714 representation, particularly during the non-growing season when they often have only one

715 monthly temporal replicate in ABCflux (McGuire et al., 2012; Fox et al., 2008). Automated
716 chamber measurements during the non-growing season are also rare in ABCflux. Furthermore,
717 uncertainty around gap-filled monthly chamber fluxes is presumably larger than that of the eddy
718 covariance because of the low temporal replication of chamber measurements. Manual chamber
719 measurements might, for example, be conducted during a limited period which does not cover
720 the range of meteorological and phenological conditions within a month. Additional uncertainties
721 in chamber measurements include, for example, accurate determination of chamber volume,
722 pressure perturbations, temperature increase during the measurement, and collars disturbing the
723 ground and causing plant root excision.

724

725 Because of these methodological differences across the eddy covariance, chamber and diffusion
726 techniques, comparing fluxes between the methods may result in inconsistencies (Fig. 7). It has
727 been shown that chamber measurements can be both larger or smaller than the fluxes estimated
728 with eddy covariance (Phillips et al., 2017). This difference can be related to the uncertainties
729 with the eddy covariance or chamber technique as described above. The differences can also be
730 due to the mismatch between the chamber and tower footprints (<1 m vs. 250–3000 m radii over
731 the measurement equipment, respectively) and the difficulty of extrapolating local chamber
732 measurements to landscape scales (Marushchak et al., 2013; Fox et al., 2008). However, several
733 studies have also shown good agreement across the eddy covariance and chamber measurements
734 (Laine et al., 2006; Wang et al., 2013; Eckhardt et al., 2019; Riutta et al., 2007). Potential
735 mismatches may also be due to a bias towards daytime measurements in manual chamber
736 measurements (see field “diurnal_coverage”). During daytime, plants are actively
737 photosynthesizing whereas respiration is the dominant flux at night (López-Blanco et al., 2017).
738 Presumably because of these day vs. night-time differences, we observed stronger sink strength
739 in manual chamber measurements compared to other flux measurements in ABCflux, even
740 though eddy covariance measurements have also been observed to underestimate night-time CO₂
741 loss. This underestimation in night-time eddy covariance measurements is due to suppressed
742 turbulent exchange linked to stable atmospheric stratification, and systematic biases due to
743 horizontal advection (Aubinet et al., 2012). Despite these uncertainties, including fluxes
744 estimated with all of these techniques into one database improves the understanding of
745 underlying variability of landscape-scale flux estimates. Indeed, there are roughly 10 sites in

746 ABCflux that include both eddy covariance and chamber/diffusion measurements conducted at
747 the same time. These observations might not have identical site coordinates but they are often
748 very close to each other (<500 m away from each other). Including multiple methods from the
749 same site provides an opportunity to compare estimates from different methods over a larger
750 number of sites.

751

752 4.2. Uncertainties in eddy covariance flux partitioning

753 Monthly Reco and GPP fluxes derived from eddy covariance were primarily estimated using
754 night-time partitioning (Reichstein et al., 2005). Focusing on night-time partitioning ensured that
755 data from older sites using this partitioning method could be included, and that most of the fluxes
756 were standardized using one common partitioning method. However, particularly at sites at
757 higher latitudes of the ABZ, low-light night-time conditions are restricted to rather short periods
758 during summer, limiting the database for assessing Reco rates and therefore increasing
759 uncertainties associated with the night-time partitioning (López-Blanco et al., 2020). Recent
760 research suggests that other methods such as daytime partitioning (Lasslop et al. 2010), and even
761 more recently artificial neural networks (ANN) (Tramontana et al., 2020), might be more
762 accurate methods for flux partitioning by addressing the assumptions from night-time
763 partitioning methods (Pastorello et al., 2020; Papale et al., 2006; Reichstein et al., 2005; Keenan
764 et al., 2019). Specifically, the assumption of a constant diel temperature sensitivity during night-
765 and daytime might introduce error in eddy covariance-based Reco estimates extrapolated from
766 night-time measurements (Järveoja et al., 2020; Keenan et al., 2019). It should be noted that
767 ABCflux database used night-time partitioning of fluxes extracted from repositories for
768 consistency; however, fluxes contributed by some databases, PIs or extracted from papers may
769 be based on other partitioning methods, as noted in the database. In a few cases, observations
770 from the same site were based on different partitioning methods, which limits the usage of data
771 at those sites for time-series exploration. These different gap-filling and partitioning approaches
772 can impact the magnitude of monthly CO₂ budgets. For example, a study comparing four gap-
773 filling methods in a boreal forest showed that the 14-year average annual NEE budget varied
774 from 4 to 48 g C m⁻² year⁻¹ depending on the gap-filling approach (Soloway et al., 2017).
775 However, a comparison of multiple gap-filling and partitioning methods across sites showed that

776 variation in annual GPP and Reco between partitioning methods was small (Desai et al., 2008),
777 which provides confidence in estimates from partitioned GPP and Reco components from the
778 differing methods used in this database.

779

780 Any one choice in gap-filling and partitioning introduces uncertainties, and to understand and
781 minimize those uncertainties remains an important research priority. However, since this
782 database was not designed for detailed explorations of how the different gap-filling and
783 partitioning approaches influence fluxes, we recommend users interested in those to access these
784 data in flux repositories or contact site PIs. Fluxes calculated using multiple gap-filling
785 techniques may be considered in the next versions of ABCflux. We further suggest data users
786 remain cautious when using ABCflux data to understand mechanistic relationships between
787 meteorological variables and fluxes, as the gap-filled and partitioned monthly fluxes already
788 include some information about, for example, air or soil temperatures and light conditions. To
789 completely avoid circularity in these exploratory analyses, we recommend data users download
790 the original and non-gap filled NEE records, or download fluxes partitioned in a way that is
791 consistent and biologically relevant for the particular research question from flux repositories.

792

793 4.3. Representativeness and completeness of the data

794 The ABCflux database site distribution covers all vegetation types and countries within the ABZ.
795 However, there are regional and temporal biases in the database due to the differences in
796 accessibility for sampling certain regions (also documented in [\(Virkkala et al. 2019; Pallandt et](#)
797 [al. 2021\)](#)). As a result, the number of monthly observations does not always correlate with the
798 size of the country/region or vegetation type. For example, Russia and Canada cover in total ca.
799 80 % of the ABZ but include only ca. 40 % of the monthly observations. While the distribution
800 of these measurements are rather balanced between the Russian tundra and boreal biomes,
801 Canadian observations are primarily located in the boreal biome, largely due to the high amount
802 of measurements conducted as part of the NASA Boreal Ecosystem-Atmosphere Study (Sellers
803 et al., 1997). Deciduous needleleaf (i.e., larch) forests, the primary vegetation type in central and
804 eastern Siberia, has the smallest amount of data compared to its area (<5 % of monthly
805 observations vs. >20 % coverage of the ABZ). Additional data gaps are located in barren and

806 prostrate-shrub tundra and sparse boreal vegetation, as well as in areas with high precipitation.
807 Eddy covariance towers in mountainous regions are also rare (Pallandt et al. 2021) as eddy
808 covariance towers are most often set up over homogeneous and flat terrains to avoid advection
809 (Baldocchi, 2003; Etzold et al., 2010). Alaska and Finland cover <10 % of the ABZ but include
810 >40 % of the monthly observations.

811
812 There are differences in environmental coverage of ABCflux depending on the measured flux,
813 measurement year, and the measurement season. Sites with NEE observations have the largest
814 geographical coverage, with less availability for partitioned GPP and Reco fluxes. Therefore,
815 regional summaries of Reco and GPP do not sum up to NEE. Moreover, although the oldest
816 records in ABCflux originate from 1989, observations from the 1990s are primarily located in a
817 few boreal or Alaskan tundra sites. The measurement records from tundra sites are shorter than
818 boreal sites over the full time span of the database, and it is therefore more uncertain to
819 investigate long-term temporal changes in tundra fluxes. Finally, the lowest amount of flux data
820 in ABCflux is during winter, which is the most challenging period for data collection in high
821 latitudes (Kittler et al., 2017b; Jentsch et al., 2021). Autumn and winter data included in
822 ABCflux further covers a smaller Arctic-Boreal climate space, with no data coming from
823 extremely cold or wet conditions (Fig. 5). Fluxes are generally small during this period (Natali et
824 al., 2019a), leading to higher relative uncertainties in flux estimation compared to other seasons.
825 These regional and temporal biases need to be considered in future analyses to assure the
826 robustness of our understanding of carbon fluxes across the ABZ.

827
828 Although ABCflux includes a comprehensive compilation of flux and supporting environmental
829 and methodological information, the information is not exhaustive. We acknowledge that this
830 database is missing some eddy covariance sites that were recently summarized in a tower survey
831 (see preliminary results in <https://cosima.nceas.ucsb.edu/carbon-flux-sites/>), because these data
832 were unavailable at the time of database compilation. Moreover, the overall quality or the gap-
833 filled percentage of the eddy covariance observations is not reported for each eddy covariance
834 site, limiting the potential to explore the effects of data quality on fluxes across all the eddy
835 covariance sites. Comparing soil temperature or moisture across sites has uncertainties due to
836 differences in sensor depths, which are not always reported in the database. We hope to improve

837 and increase the flux and supporting data in the future as new data are being collected, for
838 example, by leveraging the ONEflux pipeline and its different outputs (Pastorello et al., 2020), as
839 well as aggregating new measurements that are not part of any networks.

840 5. Data use guidelines

841 Data are publicly available using a Creative Commons Attribution 4.0 International copyright
842 (CC BY 4.0). Data are fully public, but should be appropriately referenced by citing this paper
843 and the database (see Section 6). We suggest that researchers planning to use this database as a
844 core dataset for their analysis contact and collaborate with the database developers and relevant
845 individual site contributors.

846 6. Data availability and access

847 The database associated with this publication can be found at Virkkala et al. 2021a
848 (<https://doi.org/10.3334/ORNLDAAAC/1934>).

849 7. Conclusions

850 ABCflux provides the most comprehensive database of ABZ terrestrial ecosystem CO₂ fluxes to
851 date. It is particularly useful for future modeling, remote sensing, and empirical studies aiming to
852 understand CO₂ budgets and regional variability in flux magnitudes, as well as changes in fluxes
853 through time. It can also be used to understand how different environmental conditions influence
854 fluxes, and to better understand the current extent of the flux measurement network and its
855 representativeness across the Arctic-Boreal region.

856 8. Author contributions

857 The ABCflux database was conceptualized and developed by a team led by SMN, BMR, JDW,
858 MM, AMV, and EAGS, with additional comments from OS. KS and SJC compiled the data, with
859 contributions from AMV, MM, DP, CM, and JN, and data screening by AMV and SMN. AMV
860 drafted and coordinated the manuscript in close collaboration with SMN, BMR, JDW, KS, and
861 MM. All authors contributed to the realization of the ABCflux database and participated in the
862 editing of the manuscript. PIs whose data were extracted from publications are not coauthors in
863 this paper, unless new data were provided, but their contact details can be found in the database.

864 9. Competing interests

865 The authors declare that they have no conflict of interest.

866 10. Acknowledgements

867 AMV, BMR, SMN, and JDW were funded by the Gordon and Betty Moore Foundation (grant
868 #8414). BMR, KS, SJC, CM, and JN were also funded by the NASA Carbon Cycle Science and
869 Arctic-Boreal Vulnerability Experiment programs (ABoVE grant NNX17AE13G), SMN by
870 NASA ABoVE (grant NNX15AT81A) and JDW by NNX15AT81A and NASA NIP grant
871 NNH17ZDA001N. EAGS acknowledges NSF Research, Synthesis, and Knowledge Transfer in a
872 Changing Arctic: Science Support for the Study of Environmental Arctic Change (grant
873 #1331083) and NSF PLR Arctic System Science Research Networking Activities (Permafrost
874 Carbon Network: Synthesizing Flux Observations for Benchmarking Model Projections of
875 Permafrost Carbon Exchange; grant #1931333. EAGS further acknowledges US Department of
876 Energy and Denali National Park. MBN and MP acknowledge Swedish ICOS (Integrated Carbon
877 Observatory System) funded by VR and contributing institutions; SITES (Swedish Infrastructure
878 for Ecosystem Science) funded by VR and contributing institutions; VR (grant # 2018-03966 and
879 # 2019-04676), FORMAS (grant # 2016-01289), and Kempe Foundations (SMK-1211). EE, CE,
880 and MSB-H was funded by NSF Arctic Observatory Network and CAG, VSL, EH by Natural
881 Sciences and Engineering Research Council. IM, PK, EST, AL acknowledges ICOS-Finland and
882 AV Russian Science Foundation, project 21-14-00209. AL, MA, TL, J-PT, and JH further
883 acknowledge Ministry of transport and communication. WQ, EE, VSL were funded by
884 ArcticNet. HK acknowledges The Arctic Challenge for Sustainability and The Arctic Challenge
885 for Sustainability II (JPMXD1420318865), MEM the Academy of Finland project PANDA
886 (decision no. 317054) and CV the Academy of Finland project MUFFIN (decision no. 332196).
887 NN acknowledges Arctic Data Center, National Science Foundation, US Department of Energy,
888 Denali National Park. YM was funded by Ministry of Environment, Japan and MU by the Arctic
889 Challenge for Sustainability II (ArCS II; JPMXD1420318865) and KAKENHI (19H05668).
890 SFO acknowledges US National Science Foundation, and MiM, BE, TRC Greenland Ecosystem
891 Monitoring program. BE further acknowledge Arctic Station, University of Copenhagen and the
892 Danish National Research Foundation (CENPERM D NRF100). ELB was funded by "Greenland
893 Research Council, grant number 80.35, financed by the "Danish Program for Arctic Research",

894 and LM by TCOS Siberia. DH and LK were funded by Deutsche Forschungsgemeinschaft under
895 Germany's Excellence Strategy – EXC 177 'CliSAP - Integrated Climate System Analysis and
896 Prediction'. JJ acknowledges Swedish Forest Society Foundation (2018-485-Steg 2 2017) and
897 FORMAS (2018-00792). DZ was funded by National Science Foundation (NSF) (award number
898 1204263, and 1702797) NASA ABoVE (NNX15AT74A; NNX16AF94A) Program, Natural
899 Environment Research Council (NERC) UAMS Grant (NE/P002552/1), NOAA Cooperative
900 Science Center for Earth System Sciences and Remote Sensing Technologies (NOAA-
901 CESSRST) under the Cooperative Agreement Grant # NA16SEC4810008, European Union's
902 Horizon 2020 research and innovation program under grant agreement No. 72789. S-JP was
903 funded by National Research Foundation of Korea Grant from the Korean Government (NRF-
904 2021M1A5A1065425, KOPRI-PN21011). NC acknowledges "National Research Foundation of
905 Korea Grant from the Korean Government (MSIT; the Ministry of Science and ICT) (NRF-
906 2021M1A5A1065679 and NRF-2021R1I1A1A01053870)". SD was funded by Department of
907 Energy and Ngee- Arctic. FJWP is funded by the Swedish Research Council (registration nr.
908 2017-05268) and the Research Council of Norway (grant no. 274711). ASP and VIZ were
909 funded by grant of the Russian Fund for Basic Research # 18-05-60203-Arktika. The authors
910 would like to acknowledge Tiffany Windholz for her work on standardizing and cleaning up the
911 database.

912 References

913 Abatzoglou, J. T., Dobrowski, S. Z., Parks, S. A., and Hegewisch, K. C.: TerraClimate, a high-
914 resolution global dataset of monthly climate and climatic water balance from 1958-2015, *Sci*
915 *Data*, 5, 170191, <https://doi.org/10.1038/sdata.2017.191>, 2018.

916 Natural Earth - Free vector and raster map data at 1:10m, 1:50m, and 1:110m scales:
917 <https://www.naturalearthdata.com/>, last access: 12 February 2021.

918 Reconciling historical and contemporary trends in terrestrial carbon exchange of the northern
919 permafrost-zone: [https://arcticdata.io/reconciling-historical-and-contemporary-trends-in-](https://arcticdata.io/reconciling-historical-and-contemporary-trends-in-terrestrial-carbon-exchange-of-the-northern-permafrost-zone/)
920 [terrestrial-carbon-exchange-of-the-northern-permafrost-zone/](https://arcticdata.io/reconciling-historical-and-contemporary-trends-in-terrestrial-carbon-exchange-of-the-northern-permafrost-zone/), last access: 11 February 2021.

921 Aubinet, M., Vesala, T., and Papale, D.: *Eddy Covariance: A Practical Guide to Measurement*
922 *and Data Analysis*, Springer Science & Business Media, 438 pp., 2012.

923 Aurela, M., Laurila, T., and Tuovinen, J. P.: Annual CO₂ balance of a subarctic fen in northern
924 Europe: Importance of the wintertime efflux, *J. Geophys. Res.*, 2002.

- 925 Bäckstrand, K., Crill, P. M., Jackowicz-Korczyński, M., Mastepanov, M., Christensen, T. R., and
926 Bastviken, D.: Annual carbon gas budget for a subarctic peatland, Northern Sweden,
927 <https://doi.org/10.5194/bg-7-95-2010>, 2010.
- 928 Baldocchi, D.: “Breathing” of the terrestrial biosphere: lessons learned from a global network of
929 carbon dioxide flux measurement systems, *Aust. J. Bot.*, 56, 1–26, 2008.
- 930 Baldocchi, D., Falge, E., Gu, L., Olson, R., Hollinger, D., Running, S., Anthoni, P., Bernhofer,
931 C., Davis, K., Evans, R., Fuentes, J., Goldstein, A., Katul, G., Law, B., Lee, X., Malhi, Y.,
932 Meyers, T., Munger, W., Oechel, W., Paw U, K. T., Pilegaard, K., Schmid, H. P., Valentini, R.,
933 Verma, S., Vesala, T., Wilson, K., and Wofsy, S.: FLUXNET: A New Tool to Study the
934 Temporal and Spatial Variability of Ecosystem-Scale Carbon Dioxide, Water Vapor, and Energy
935 Flux Densities, *Bull. Am. Meteorol. Soc.*, 82, 2415–2434, [https://doi.org/10.1175/1520-0477\(2001\)082<2415:FANTTS>2.3.CO;2](https://doi.org/10.1175/1520-0477(2001)082<2415:FANTTS>2.3.CO;2), 2001.
- 937 Baldocchi, D., Chu, H., and Reichstein, M.: Inter-annual variability of net and gross ecosystem
938 carbon fluxes: A review, *Agric. For. Meteorol.*, 249, 520–533,
939 <https://doi.org/10.1016/j.agrformet.2017.05.015>, 2018.
- 940 Baldocchi, D. D.: Assessing the eddy covariance technique for evaluating carbon dioxide
941 exchange rates of ecosystems: past, present and future, <https://doi.org/10.1046/j.1365-2486.2003.00629.x>, 2003.
- 943 Belshe, E. F., Schuur, E. A. G., and Bolker, B. M.: Tundra ecosystems observed to be CO₂
944 sources due to differential amplification of the carbon cycle, *Ecol. Lett.*, 16, 1307–1315,
945 <https://doi.org/10.1111/ele.12164>, 2013.
- 946 Björkman, M. P., Morgner, E., Björk, R. G., Cooper, E. J., Elberling, B., and Klemetsson, L.: A
947 comparison of annual and seasonal carbon dioxide effluxes between sub-Arctic Sweden and
948 High-Arctic Svalbard, *Polar Res.*, 29, 75–84, <https://doi.org/10.1111/j.1751-8369.2010.00150.x>,
949 2010a.
- 950 Björkman, M. P., Morgner, E., Cooper, E. J., Elberling, B., Klemetsson, L., and Björk, R. G.:
951 Winter carbon dioxide effluxes from Arctic ecosystems: An overview and comparison of
952 methodologies: WINTER CO₂EFFLUXES FROM ARCTIC SOILS, *Global Biogeochem.*
953 *Cycles*, 24, <https://doi.org/10.1029/2009gb003667>, 2010b.
- 954 Bond-Lamberty, B., Christianson, D. S., Malhotra, A., Pennington, S. C., Sihi, D.,
955 AghaKouchak, A., Anjileli, H., Altaf Arain, M., Armesto, J. J., Ashraf, S., Ataka, M., Baldocchi,
956 D., Andrew Black, T., Buchmann, N., Carbone, M. S., Chang, S.-C., Crill, P., Curtis, P. S.,
957 Davidson, E. A., Desai, A. R., Drake, J. E., El-Madany, T. S., Gavazzi, M., Görres, C.-M.,
958 Gough, C. M., Goulden, M., Gregg, J., Gutiérrez Del Arroyo, O., He, J.-S., Hirano, T., Hoppie,
959 A., Hughes, H., Järveoja, J., Jassal, R., Jian, J., Kan, H., Kaye, J., Kominami, Y., Liang, N.,
960 Lipson, D., Macdonald, C. A., Maseyk, K., Mathes, K., Mauritz, M., Mayes, M. A., McNulty, S.,
961 Miao, G., Migliavacca, M., Miller, S., Miniati, C. F., Nietz, J. G., Nilsson, M. B., Noormets, A.,
962 Norouzi, H., O’Connell, C. S., Osborne, B., Oyonarte, C., Pang, Z., Peichl, M., Pendall, E.,
963 Perez-Quezada, J. F., Phillips, C. L., Phillips, R. P., Raich, J. W., Renchon, A. A., Ruehr, N. K.,
964 Sánchez-Cañete, E. P., Saunders, M., Savage, K. E., Schrumppf, M., Scott, R. L., Seibt, U., Silver,

- 965 W. L., Sun, W., Szutu, D., Takagi, K., Takagi, M., Teramoto, M., Tjoelker, M. G., Trumbore, S.,
966 Ueyama, M., Vargas, R., Varner, R. K., Verfaillie, J., Vogel, C., Wang, J., Winston, G., Wood,
967 T. E., Wu, J., Wutzler, T., Zeng, J., Zha, T., Zhang, Q., and Zou, J.: COSORE: A community
968 database for continuous soil respiration and other soil-atmosphere greenhouse gas flux data,
969 *Glob. Chang. Biol.*, 26, 7268–7283, <https://doi.org/10.1111/gcb.15353>, 2020.
- 970 Box, J. E., Colgan, W. T., Christensen, T. R., Schmidt, N. M., Lund, M., Parmentier, F.-J. W.,
971 Brown, R., Bhatt, U. S., Euskirchen, E. S., Romanovsky, V. E., Walsh, J. E., Overland, J. E.,
972 Wang, M., Corell, R. W., Meier, W. N., Wouters, B., Mernild, S., Mård, J., Pawlak, J., and
973 Olsen, M. S.: Key indicators of Arctic climate change: 1971–2017, *Environ. Res. Lett.*, 14,
974 045010, <https://doi.org/10.1088/1748-9326/aafc1b>, 2019.
- 975 Cahoon, S. M. P., Sullivan, P. F., and Post, E.: Greater Abundance of *Betula nana* and Early
976 Onset of the Growing Season Increase Ecosystem CO₂ Uptake in West Greenland, *Ecosystems*,
977 19, 1149–1163, <https://doi.org/10.1007/s10021-016-9997-7>, 2016.
- 978 Chu, H., Luo, X., Ouyang, Z., Chan, W. S., Dengel, S., Biraud, S. C., Torn, M. S., Metzger, S.,
979 Kumar, J., Arain, M. A., Arkebauer, T. J., Baldocchi, D., Bernacchi, C., Billesbach, D., Black, T.
980 A., Blanken, P. D., Bohrer, G., Bracho, R., Brown, S., Brunsell, N. A., Chen, J., Chen, X., Clark,
981 K., Desai, A. R., Duman, T., Durden, D., Fares, S., Forbrich, I., Gamon, J. A., Gough, C. M.,
982 Griffis, T., Helbig, M., Hollinger, D., Humphreys, E., Ikawa, H., Iwata, H., Ju, Y., Knowles, J.
983 F., Knox, S. H., Kobayashi, H., Kolb, T., Law, B., Lee, X., Litvak, M., Liu, H., Munger, J. W.,
984 Noormets, A., Novick, K., Oberbauer, S. F., Oechel, W., Oikawa, P., Papuga, S. A., Pendall, E.,
985 Prajapati, P., Prueger, J., Quinton, W. L., Richardson, A. D., Russell, E. S., Scott, R. L., Starr,
986 G., Staebler, R., Stoy, P. C., Stuart-Haëntjens, E., Sonnentag, O., Sullivan, R. C., Suyker, A.,
987 Ueyama, M., Vargas, R., Wood, J. D., and Zona, D.: Representativeness of Eddy-Covariance
988 flux footprints for areas surrounding AmeriFlux sites, *Agric. For. Meteorol.*, 301-302, 108350,
989 <https://doi.org/10.1016/j.agrformet.2021.108350>, 2021.
- 990 Desai, A. R., Richardson, A. D., Moffat, A. M., Kattge, J., Hollinger, D. Y., Barr, A., Falge, E.,
991 Noormets, A., Papale, D., Reichstein, M., and Stauch, V. J.: Cross-site evaluation of eddy
992 covariance GPP and RE decomposition techniques, *Agric. For. Meteorol.*, 148, 821–838,
993 <https://doi.org/10.1016/j.agrformet.2007.11.012>, 2008.
- 994 Didan, K.: MOD13A3 MODIS/Terra Vegetation Indices Monthly L3 Global 1km SIN Grid
995 V006, <https://doi.org/10.5067/MODIS/MOD13A3.006>, 2015.
- 996 Dinerstein, E., Olson, D., Joshi, A., Vynne, C., Burgess, N. D., Wikramanayake, E., Hahn, N.,
997 Palminteri, S., Hedao, P., Noss, R., Hansen, M., Locke, H., Ellis, E. C., Jones, B., Barber, C. V.,
998 Hayes, R., Kormos, C., Martin, V., Crist, E., Sechrest, W., Price, L., Baillie, J. E. M., Weeden,
999 D., Suckling, K., Davis, C., Sizer, N., Moore, R., Thau, D., Birch, T., Potapov, P., Turubanova,
1000 S., Tyukavina, A., de Souza, N., Pinteá, L., Brito, J. C., Llewellyn, O. A., Miller, A. G., Patzelt,
1001 A., Ghazanfar, S. A., Timberlake, J., Klöser, H., Shennan-Farpón, Y., Kindt, R., Lillesø, J.-P. B.,
1002 van Breugel, P., Graudal, L., Vogé, M., Al-Shammari, K. F., and Saleem, M.: An Ecoregion-
1003 Based Approach to Protecting Half the Terrestrial Realm, *Bioscience*, 67, 534–545,
1004 <https://doi.org/10.1093/biosci/bix014>, 2017.

- 1005 Eckhardt, T., Knoblauch, C., Kutzbach, L., Holl, D., Simpson, G., Abakumov, E., and Pfeiffer,
1006 E.-M.: Partitioning net ecosystem exchange of CO₂ on the pedon scale in the Lena River Delta,
1007 Siberia, *Biogeosciences*, 16, 1543–1562, <https://doi.org/10.5194/bg-16-1543-2019>, 2019.
- 1008 Etzold, S., Buchmann, N., and Eugster, W.: Contribution of advection to the carbon budget
1009 measured by eddy covariance at a steep mountain slope forest in Switzerland, *Biogeosciences*, 7,
1010 2461–2475, <https://doi.org/10.5194/bg-7-2461-2010>, 2010.
- 1011 Euskirchen, E. S., Bret-Harte, M. S., Scott, G. J., Edgar, C., and Shaver, G. R.: Seasonal patterns
1012 of carbon dioxide and water fluxes in three representative tundra ecosystems in northern Alaska,
1013 *Ecosphere*, 3, art4, <https://doi.org/10.1890/es11-00202.1>, 2012.
- 1014 Fox, A. M., Huntley, B., Lloyd, C. R., Williams, M., and Baxter, R.: Net ecosystem exchange
1015 over heterogeneous Arctic tundra: Scaling between chamber and eddy covariance measurements,
1016 *Global Biogeochem. Cycles*, 22, 2008.
- 1017 Gorham, E.: Northern Peatlands: Role in the Carbon Cycle and Probable Responses to Climatic
1018 Warming, *Ecol. Appl.*, 1, 182–195, <https://doi.org/10.2307/1941811>, 1991.
- 1019 Hari, P., Nikinmaa, E., Pohja, T., Siivola, E., Bäck, J., Vesala, T., and Kulmala, M.: Station for
1020 Measuring Ecosystem-Atmosphere Relations: SMEAR, in: *Physical and Physiological Forest
1021 Ecology*, edited by: Hari, P., Heliövaara, K., and Kulmala, L., Springer Netherlands, Dordrecht,
1022 471–487, https://doi.org/10.1007/978-94-007-5603-8_9, 2013.
- 1023 Hayes, D. J., Kicklighter, D. W., David McGuire, A., Chen, M., Zhuang, Q., Yuan, F., Melillo, J.
1024 M., and Wullschleger, S. D.: The impacts of recent permafrost thaw on land–atmosphere
1025 greenhouse gas exchange, *Environ. Res. Lett.*, 9, 045005, <https://doi.org/10.1088/1748-9326/9/4/045005>, 2014.
- 1027 Heiskanen, L., Tuovinen, J.-P., Räsänen, A., Virtanen, T., Juutinen, S., Lohila, A., Penttilä, T.,
1028 Linkosalmi, M., Mikola, J., Laurila, T., and Aurela, M.: Carbon dioxide and methane exchange
1029 of a patterned subarctic fen during two contrasting growing seasons, *Biogeosciences*, 18, 873–
1030 896, <https://doi.org/10.5194/bg-18-873-2021>, 2021.
- 1031 Helbig, M., Wischnewski, K., Gosselin, G. H., Biraud, S. C., Bogoev, I., Chan, W. S.,
1032 Euskirchen, E. S., Glenn, A. J., Marsh, P. M., Quinton, W. L., and Sonntag, O.: Addressing a
1033 systematic bias in carbon dioxide flux measurements with the EC150 and the IRGASON open-
1034 path gas analyzers, *Agric. For. Meteorol.*, 228–229, 349–359,
1035 <https://doi.org/10.1016/j.agrformet.2016.07.018>, 2016.
- 1036 Heliasz, M., Johansson, T., Lindroth, A., Mölder, M., Mastepanov, M., Friborg, T., Callaghan, T.
1037 V., and Christensen, T. R.: Quantification of C uptake in subarctic birch forest after setback by
1038 an extreme insect outbreak, *Geophys. Res. Lett.*, 38, <https://doi.org/10.1029/2010gl044733>,
1039 2011.
- 1040 Hermle, S., Lavigne, M. B., Bernier, P. Y., Bergeron, O., and Paré, D.: Component respiration,
1041 ecosystem respiration and net primary production of a mature black spruce forest in northern
1042 Quebec, *Tree Physiol.*, 30, 527–540, <https://doi.org/10.1093/treephys/tpq002>, 2010.

- 1043 Hugelius, G., Strauss, J., Zubrzycki, S., Harden, J. W., Schuur, E. A. G., Ping, C.-L.,
1044 Schirrmeister, L., Grosse, G., Michaelson, G. J., Koven, C. D., and Others: Estimated stocks of
1045 circumpolar permafrost carbon with quantified uncertainty ranges and identified data gaps,
1046 *Biogeosciences*, 11, 2014.
- 1047 Hugelius, G., Loisel, J., Chadburn, S., Jackson, R. B., Jones, M., MacDonald, G., Marushchak,
1048 M., Olefeldt, D., Packalen, M., Siewert, M. B., Treat, C., Turetsky, M., Voigt, C., and Yu, Z.:
1049 Large stocks of peatland carbon and nitrogen are vulnerable to permafrost thaw, *Proc. Natl.*
1050 *Acad. Sci. U. S. A.*, 117, 20438–20446, <https://doi.org/10.1073/pnas.1916387117>, 2020.
- 1051 Järveoja, J., Nilsson, M. B., Gažovič, M., Crill, P. M., and Peichl, M.: Partitioning of the net CO
1052 2 exchange using an automated chamber system reveals plant phenology as key control of
1053 production and respiration fluxes in a boreal peatland, *Glob. Chang. Biol.*, 24, 3436–3451, 2018.
- 1054 Järveoja, J., Nilsson, M. B., Crill, P. M., and Peichl, M.: Bimodal diel pattern in peatland
1055 ecosystem respiration rebuts uniform temperature response, *Nat. Commun.*, 11, 4255,
1056 <https://doi.org/10.1038/s41467-020-18027-1>, 2020.
- 1057 Jentzsch, K., Schulz, A., Pirk, N., Foken, T., Crewell, S., and Boike, J.: High levels of CO 2
1058 exchange during synoptic-scale events introduce large uncertainty into the arctic carbon budget,
1059 *Geophys. Res. Lett.*, 48, <https://doi.org/10.1029/2020gl092256>, 2021.
- 1060 Jian, J., Vargas, R., Anderson-Teixeira, K., Stell, E., Herrmann, V., Horn, M., Kholod, N.,
1061 Manzon, J., Marchesi, R., Paredes, D., and Others: A restructured and updated global soil
1062 respiration database (SRDB-V5), 1–19, 2020.
- 1063 Keenan, T. F. and Williams, C. A.: The Terrestrial Carbon Sink, *Annu. Rev. Environ. Resour.*,
1064 43, 219–243, <https://doi.org/10.1146/annurev-environ-102017-030204>, 2018.
- 1065 Keenan, T. F., Migliavacca, M., Papale, D., Baldocchi, D., Reichstein, M., Torn, M., and
1066 Wutzler, T.: Widespread inhibition of daytime ecosystem respiration, *Nat Ecol Evol*, 3, 407–415,
1067 <https://doi.org/10.1038/s41559-019-0809-2>, 2019.
- 1068 Kittler, F., Eugster, W., Foken, T., Heimann, M., Kolle, O., and Göckede, M.: High-quality
1069 eddy-covariance CO2 budgets under cold climate conditions: Arctic Eddy-Covariance
1070 CO2 Budgets, *J. Geophys. Res. Biogeosci.*, 122, 2064–2084,
1071 <https://doi.org/10.1002/2017jg003830>, 2017a.
- 1072 Kittler, F., Heimann, M., Kolle, O., Zimov, N., Zimov, S., and Göckede, M.: Long-term drainage
1073 reduces CO2 uptake and CH4 emissions in a Siberian permafrost ecosystem, *Global*
1074 *Biogeochem. Cycles*, 31, 1704–1717, 2017b.
- 1075 Lafleur, P. M., Humphreys, E. R., St Louis, V. L., Myklebust, M. C., Papakyriakou, T., Poissant,
1076 L., Barker, J. D., Pilote, M., and Swystun, K. A.: Variation in peak growing season net
1077 ecosystem production across the Canadian Arctic, *Environ. Sci. Technol.*, 46, 7971–7977,
1078 <https://doi.org/10.1021/es300500m>, 2012.
- 1079 Laine, A., Sottocornola, M., Kiely, G., Byrne, K. A., Wilson, D., and Tuittila, E.-S.: Estimating

- 1080 net ecosystem exchange in a patterned ecosystem: Example from blanket bog, *Agric. For.*
1081 *Meteorol.*, 138, 231–243, <https://doi.org/10.1016/j.agrformet.2006.05.005>, 2006.
- 1082 Lamarche, C., Bontemps, S., Verhegghen, A., Radoux, J., Vanbogaert, E., Kalogirou, V., Seifert,
1083 F. M., Arino, O., and Defourny, P.: Characterizing The Surface Dynamics For Land Cover
1084 Mapping: Current Achievements Of The ESA CCI Land Cover, 72279, 2013.
- 1085 Lasslop, G., Reichstein, M., Papale, D., Richardson, A. D., Arneth, A., Barr, A., Stoy, P., and
1086 Wohlfahrt, G.: Separation of net ecosystem exchange into assimilation and respiration using a
1087 light response curve approach: critical issues and global evaluation: SEPARATION OF NEE
1088 INTO GPP AND RECO, *Glob. Chang. Biol.*, 16, 187–208, [https://doi.org/10.1111/j.1365-](https://doi.org/10.1111/j.1365-2486.2009.02041.x)
1089 [2486.2009.02041.x](https://doi.org/10.1111/j.1365-2486.2009.02041.x), 2010.
- 1090 López-Blanco, E., Lund, M., Williams, M., Tamstorf, M. P., Westergaard-Nielsen, A., Exbrayat,
1091 J.-F., Hansen, B. U., and Christensen, T. R.: Exchange of CO₂ in Arctic tundra: impacts of
1092 meteorological variations and biological disturbance, *Biogeosciences*, 14, 4467–4483,
1093 <https://doi.org/10.5194/bg-14-4467-2017>, 2017.
- 1094 López-Blanco, E., Jackowicz-Korczynski, M., Mastepanov, M., Skov, K., Westergaard-Nielsen,
1095 A., Williams, M., and Christensen, T. R.: Multi-year data-model evaluation reveals the
1096 importance of nutrient availability over climate in arctic ecosystem C dynamics, *Environ. Res.*
1097 *Let.*, 15, 094007, <https://doi.org/10.1088/1748-9326/ab865b>, 2020.
- 1098 Luysaert, S., Inglima, I., Jung, M., Richardson, A. D., Reichstein, M., Papale, D., Piao, S. L.,
1099 Schulze, E.-D., Wingate, L., Matteucci, G., Aragao, L., Aubinet, M., Beer, C., Bernhofer, C.,
1100 Black, K. G., Bonal, D., Bonnefond, J.-M., Chambers, J., Ciais, P., Cook, B., Davis, K. J.,
1101 Dolman, A. J., Gielen, B., Goulden, M., Grace, J., Granier, A., Grelle, A., Griffis, T., Grünwald,
1102 T., Guidolotti, G., Hanson, P. J., Harding, R., Hollinger, D. Y., Hutyrá, L. R., Kolari, P., Kruijt,
1103 B., Kutsch, W., Lagergren, F., Laurila, T., Law, B. E., Le Maire, G., Lindroth, A., Loustau, D.,
1104 Malhi, Y., Mateus, J., Migliavacca, M., Misson, L., Montagnani, L., Moncrieff, J., Moors, E.,
1105 Munger, J. W., Nikinmaa, E., Ollinger, S. V., Pita, G., Rebmann, C., Rouspard, O., Saigusa, N.,
1106 Sanz, M. J., Seufert, G., Sierra, C., Smith, M.-L., Tang, J., Valentini, R., Vesala, T., and
1107 Janssens, I. A.: CO₂ balance of boreal, temperate, and tropical forests derived from a global
1108 database, *Glob. Chang. Biol.*, 13, 2509–2537, <https://doi.org/10.1111/j.1365-2486.2007.01439.x>,
1109 2007.
- 1110 Marushchak, M. E., Kiepe, I., Biasi, C., Elsakov, V., Friborg, T., Johansson, T., Soegaard, H.,
1111 Virtanen, T., and Martikainen, P. J.: Carbon dioxide balance of subarctic tundra from plot to
1112 regional scales, <https://doi.org/10.5194/bg-10-437-2013>, 2013.
- 1113 McGuire, A. D., Christensen, T. R., Hayes, D. J., Heroult, A., Euskirchen, E., Yi, Y., Kimball, J.
1114 S., Koven, C., Lafleur, P., Miller, P. A., Oechel, W., Peylin, P., and Williams, M.: An assessment
1115 of the carbon balance of arctic tundra: comparisons among observations, process models, and
1116 atmospheric inversions, *Biogeosci. Discuss.*, 9, 4543, <https://doi.org/10.5194/bg-9-3185-2012>,
1117 2012.
- 1118 McGuire, A. D., Koven, C., Lawrence, D. M., Klein, J. S., Xia, J., Beer, C., Burke, E., Chen, G.,
1119 Chen, X., Delire, C., Jafarov, E., MacDougall, A. H., Marchenko, S., Nicolsky, D., Peng, S.,

- 1120 Rinke, A., Saito, K., Zhang, W., Alkama, R., Bohn, T. J., Ciais, P., Decharme, B., Ekici, A.,
1121 Gouttevin, I., Hajima, T., Hayes, D. J., Ji, D., Krinner, G., Lettenmaier, D. P., Luo, Y., Miller, P.
1122 A., Moore, J. C., Romanovsky, V., Schädel, C., Schaefer, K., Schuur, E. A. G., Smith, B.,
1123 Sueyoshi, T., and Zhuang, Q.: Variability in the sensitivity among model simulations of
1124 permafrost and carbon dynamics in the permafrost region between 1960 and 2009, *Global*
1125 *Biogeochem. Cycles*, 30, 1015–1037, <https://doi.org/10.1002/2016GB005405>, 2016.
- 1126 Merbold, L., Kutsch, W. L., Corradi, C., Kolle, O., Rebmann, C., Stoy, P. C., Zimov, S. A., and
1127 Schulze, E.-D.: Artificial drainage and associated carbon fluxes (CO₂/CH₄) in a tundra
1128 ecosystem, *Glob. Chang. Biol.*, 15, 2599–2614, <https://doi.org/10.1111/j.1365->
1129 [2486.2009.01962.x](https://doi.org/10.1111/j.1365-2486.2009.01962.x), 2009.
- 1130 Mishra, U., Hugelius, G., Shelef, E., Yang, Y., Strauss, J., Lupachev, A., Harden, J. W., Jastrow,
1131 J. D., Ping, C.-L., Riley, W. J., Schuur, E. A. G., Matamala, R., Siewert, M., Nave, L. E., Koven,
1132 C. D., Fuchs, M., Palmtag, J., Kuhry, P., Treat, C. C., Zubrzycki, S., Hoffman, F. M., Elberling,
1133 B., Camill, P., Veremeeva, A., and Orr, A.: Spatial heterogeneity and environmental predictors
1134 of permafrost region soil organic carbon stocks, *Sci Adv*, 7,
1135 <https://doi.org/10.1126/sciadv.aaz5236>, 2021.
- 1136 Natali, S. M., Watts, J. D., Rogers, B. M., Potter, S., Ludwig, S. M., Selbmann, A.-K., Sullivan,
1137 P. F., Abbott, B. W., Arndt, K. A., Birch, L., Björkman, M. P., Bloom, A. A., Celis, G.,
1138 Christensen, T. R., Christiansen, C. T., Commane, R., Cooper, E. J., Crill, P., Czimczik, C.,
1139 Davydov, S., Du, J., Egan, J. E., Elberling, B., Euskirchen, E. S., Friborg, T., Genet, H.,
1140 Göckede, M., Goodrich, J. P., Grogan, P., Helbig, M., Jafarov, E. E., Jastrow, J. D., Kalhori, A.
1141 A. M., Kim, Y., Kimball, J. S., Kutzbach, L., Lara, M. J., Larsen, K. S., Lee, B.-Y., Liu, Z.,
1142 Lorant, M. M., Lund, M., Lupascu, M., Madani, N., Malhotra, A., Matamala, R., McFarland, J.,
1143 McGuire, A. D., Michelsen, A., Minions, C., Oechel, W. C., Olefeldt, D., Parmentier, F.-J. W.,
1144 Pirk, N., Poulter, B., Quinton, W., Rezanezhad, F., Risk, D., Sachs, T., Schaefer, K., Schmidt, N.
1145 M., Schuur, E. A. G., Semenchuk, P. R., Shaver, G., Sonntag, O., Starr, G., Treat, C. C.,
1146 Waldrop, M. P., Wang, Y., Welker, J., Wille, C., Xu, X., Zhang, Z., Zhuang, Q., and Zona, D.:
1147 Large loss of CO₂ in winter observed across the northern permafrost region, *Nat. Clim. Chang.*,
1148 9, 852–857, <https://doi.org/10.1038/s41558-019-0592-8>, 2019a.
- 1149 Natali, S., J.D. Watts, S. Potter, B.M. Rogers, S. Ludwig, A. Selbmann, P. Sullivan et al.
1150 Synthesis of winter in situ soil CO₂ flux in pan-arctic and boreal regions, 1989-2017:
1151 https://daac.ornl.gov/ABOVE/guides/Nongrowing_Season_CO2_Flux.html, 2019b.
- 1152 Nobrega, S. and Grogan, P.: Landscape and ecosystem-level controls on net carbon dioxide
1153 exchange along a natural moisture gradient in Canadian low arctic tundra, *Ecosystems*, 11, 377–
1154 396, <https://doi.org/10.1007/s10021-008-9128-1>, 2008.
- 1155 Novick, K. A., Biederman, J. A., Desai, A. R., Litvak, M. E., Moore, D. J. P., Scott, R. L., and
1156 Torn, M. S.: The AmeriFlux network: A coalition of the willing, *Agric. For. Meteorol.*, 249,
1157 444–456, <https://doi.org/10.1016/j.agrformet.2017.10.009>, 2018.
- 1158 Nykänen, H., Heikkinen, J. E. P., Pirinen, L., Tiilikainen, K., and Martikainen, P. J.: Annual
1159 CO₂ exchange and CH₄ fluxes on a subarctic palsamire during climatically different years,

- 1160 Global Biogeochem. Cycles, 17, 2003.
- 1161 Oechel, W. C., Vourlitis, G. L., Hastings, S. J., Zulueta, R. C., Hinzman, L., and Kane, D.:
 1162 Acclimation of ecosystem CO₂ exchange in the Alaskan Arctic in response to decadal climate
 1163 warming, *Nature*, 406, 978–981, <https://doi.org/10.1038/35023137>, 2000.
- 1164 Pallandt M., Kumar J., Mauritz M., et al. Representativeness assessment of the pan-Arctic eddy-
 1165 covariance site network, and optimized future enhancements. *Biogeosciences Discussions* (July):
 1166 1–42, 2021.
- 1167 Papale, D., Reichstein, M., Aubinet, M., Canfora, E., Bernhofer, C., Kutsch, W., Longdoz, B.,
 1168 Rambal, S., Valentini, R., Vesala, T., and Yakir, D.: Towards a standardized processing of Net
 1169 Ecosystem Exchange measured with eddy covariance technique: algorithms and uncertainty
 1170 estimation, *Biogeosciences*, 3, 571–583, <https://doi.org/10.5194/bg-3-571-2006>, 2006.
- 1171 Paris, J.-D., Ciais, P., Rivier, L., Chevallier, F., Dolman, H., Flaud, J.-M., Garrec, C., Gerbig, C.,
 1172 Grace, J., Huertas, E., Johannessen, T., Jordan, A., Levin, I., Papale, D., Valentini, R., Watson,
 1173 A., Vesala, T., and ICOS-PP Consortium: Integrated Carbon Observation System, 12397, 2012.
- 1174 Parker, T. C., Subke, J.-A., and Wookey, P. A.: Rapid carbon turnover beneath shrub and tree
 1175 vegetation is associated with low soil carbon stocks at a subarctic treeline, *Glob. Chang. Biol.*,
 1176 21, 2070–2081, <https://doi.org/10.1111/gcb.12793>, 2015.
- 1177 Parmentier, F.-J., Sonnentag, O., Mauritz, M., Virkkala, A.-M., and Schuur, E.: Is the northern
 1178 permafrost zone a source or a sink for carbon?, *Eos*, 100, <https://doi.org/10.1029/2019eo130507>,
 1179 2019.
- 1180 Pastorello, G., Trotta, C., Canfora, E., Chu, H., Christianson, D., Cheah, Y.-W., Poindexter, C.,
 1181 Chen, J., Elbashandy, A., Humphrey, M., Isaac, P., Polidori, D., Ribeca, A., van Ingen, C.,
 1182 Zhang, L., Amiro, B., Ammann, C., Arain, M. A., Ardö, J., Arkebauer, T., Arndt, S. K., Arriga,
 1183 N., Aubinet, M., Aurela, M., Baldocchi, D., Barr, A., Beamesderfer, E., Marchesini, L. B.,
 1184 Bergeron, O., Beringer, J., Bernhofer, C., Berveiller, D., Billesbach, D., Black, T. A., Blanken,
 1185 P. D., Bohrer, G., Boike, J., Bolstad, P. V., Bonal, D., Bonnefond, J.-M., Bowling, D. R.,
 1186 Bracho, R., Brodeur, J., Brümmer, C., Buchmann, N., Burban, B., Burns, S. P., Buysse, P., Cale,
 1187 P., Cavagna, M., Cellier, P., Chen, S., Chini, I., Christensen, T. R., Cleverly, J., Collalti, A.,
 1188 Consalvo, C., Cook, B. D., Cook, D., Coursolle, C., Cremonese, E., Curtis, P. S., D’Andrea, E.,
 1189 da Rocha, H., Dai, X., Davis, K. J., De Cinti, B., de Grandcourt, A., De Ligne, A., De Oliveira,
 1190 R. C., Delpierre, N., Desai, A. R., Di Bella, C. M., di Tommasi, P., Dolman, H., Domingo, F.,
 1191 Dong, G., Dore, S., Duce, P., Dufrêne, E., Dunn, A., Dušek, J., Eamus, D., Eichelmann, U.,
 1192 ElKhidir, H. A. M., Eugster, W., Ewenz, C. M., Ewers, B., Famulari, D., Fares, S., Feigenwinter,
 1193 I., Feitz, A., Fensholt, R., Filippa, G., Fischer, M., Frank, J., Galvagno, M., Gharun, M.,
 1194 Gianelle, D., et al.: The FLUXNET2015 dataset and the ONEFlux processing pipeline for eddy
 1195 covariance data, *Sci Data*, 7, 225, <https://doi.org/10.1038/s41597-020-0534-3>, 2020.
- 1196 Pavelka, M., Acosta, M., Kiese, R., Altimir, N., Brümmer, C., Crill, P., Darenova, E., Fuß, R.,
 1197 Gielen, B., Graf, A., Klemetsson, L., Lohila, A., Longdoz, B., Lindroth, A., Nilsson, M.,
 1198 Marañon-Jimenez, S., Merbold, L., Montagnani, L., Peichl, M., Pihlatie, M., Pumpanen, J.,
 1199 Ortiz, P. S., Silvennoinen, H., Skiba, U., Vestin, P., Weslien, P., Janouš, D., and Kutsch, W.:

- 1200 Standardisation of chamber technique for CO₂, N₂O and CH₄ fluxes measurements from
1201 terrestrial ecosystems, *Int. Agrophys.*, 32, 569–587, <https://doi.org/10.1515/intag-2017-0045>,
1202 2018.
- 1203 Phillips, C. L., Bond-Lamberty, B., Desai, A. R., Lavoie, M., Risk, D., Tang, J., Todd-Brown,
1204 K., and Vargas, R.: The value of soil respiration measurements for interpreting and modeling
1205 terrestrial carbon cycling, *Plant Soil*, 413, 1–25, <https://doi.org/10.1007/s11104-016-3084-x>,
1206 2017.
- 1207 Pirk, N., Sievers, J., Mertes, J., Parmentier, F.-J. W., Mastepanov, M., and Christensen, T. R.:
1208 Spatial variability of CO₂ uptake in polygonal tundra: assessing low-frequency disturbances in
1209 eddy covariance flux estimates, *Biogeosciences*, 14, 3157–3169, [https://doi.org/10.5194/bg-14-](https://doi.org/10.5194/bg-14-3157-2017)
1210 3157-2017, 2017.
- 1211 Reynolds, M. K., Walker, D. A., Balsler, A., Bay, C., Campbell, M., Cherosov, M. M., Daniëls,
1212 F. J. A., Eidesen, P. B., Ermokhina, K. A., Frost, G. V., Jędrzejek, B., Jorgenson, M. T.,
1213 Kennedy, B. E., Kholod, S. S., Lavrinenko, I. A., Lavrinenko, O. V., Magnússon, B., Matveyeva,
1214 N. V., Metúsalemsson, S., Nilsen, L., Olthof, I., Pospelov, I. N., Pospelova, E. B., Pouliot, D.,
1215 Razzhivin, V., Schaepman-Strub, G., Šibík, J., Telyatnikov, M. Y., and Troeva, E.: A raster
1216 version of the Circumpolar Arctic Vegetation Map (CAVM), *Remote Sens. Environ.*, 232,
1217 111297, <https://doi.org/10.1016/j.rse.2019.111297>, 2019.
- 1218 Reichstein, M., Falge, E., Baldocchi, D., Papale, D., Aubinet, M., Berbigier, P., Bernhofer, C.,
1219 Buchmann, N., Gilmanov, T., Granier, A., Grunwald, T., Havrankova, K., Ilvesniemi, H.,
1220 Janous, D., Knohl, A., Laurila, T., Lohila, A., Loustau, D., Matteucci, G., Meyers, T., Miglietta,
1221 F., Ourcival, J.-M., Pumpanen, J., Rambal, S., Rotenberg, E., Sanz, M., Tenhunen, J., Seufert,
1222 G., Vaccari, F., Vesala, T., Yakir, D., and Valentini, R.: On the separation of net ecosystem
1223 exchange into assimilation and ecosystem respiration: review and improved algorithm, *Glob.*
1224 *Chang. Biol.*, 11, 1424–1439, <https://doi.org/10.1111/j.1365-2486.2005.001002.x>, 2005.
- 1225 Riutta, T., Laine, J., Aurela, M., Rinne, J., Vesala, T., Laurila, T., Haapanala, S., Pihlatie, M.,
1226 and Tuittila, E.-S.: Spatial variation in plant community functions regulates carbon gas dynamics
1227 in a boreal fen ecosystem, *Tellus B Chem. Phys. Meteorol.*, 59, 838–852,
1228 <https://doi.org/10.1111/j.1600-0889.2007.00302.x>, 2007.
- 1229 Ryan, M. G., Lavigne, M. B., and Gower, S. T.: Annual carbon cost of autotrophic respiration in
1230 boreal forest ecosystems in relation to species and climate, *J. Geophys. Res.*, 102, 28871–28883,
1231 <https://doi.org/10.1029/97jd01236>, 1997.
- 1232 Schneider, J., Kutzbach, L., and Wilmking, M.: Carbon dioxide exchange fluxes of a boreal
1233 peatland over a complete growing season, Komi Republic, NW Russia, *Biogeochemistry*, 111,
1234 485–513, <https://doi.org/10.1007/s10533-011-9684-x>, 2012.
- 1235 Schuur, E. A. G., McGuire, A. D., Schädel, C., Grosse, G., Harden, J. W., Hayes, D. J.,
1236 Hugelius, G., Koven, C. D., Kuhry, P., Lawrence, D. M., Natali, S. M., Olefeldt, D.,
1237 Romanovsky, V. E., Schaefer, K., Turetsky, M. R., Treat, C. C., and Vonk, J. E.: Climate change
1238 and the permafrost carbon feedback, *Nature*, 520, 171–179, <https://doi.org/10.1038/nature14338>,
1239 2015.

- 1240 Sellers, P. J., Hall, F. G., Kelly, R. D., Black, A., Baldocchi, D., Berry, J., Ryan, M., Ranson, K.
1241 J., Crill, P. M., Lettenmaier, D. P., Margolis, H., Cihlar, J., Newcomer, J., Fitzjarrald, D., Jarvis,
1242 P. G., Gower, S. T., Halliwell, D., Williams, D., Goodison, B., Wickland, D. E., and Guertin, F.
1243 E.: BOREAS in 1997: Experiment overview, scientific results, and future directions, *J. Geophys.*
1244 *Res.*, 102, 28731–28769, <https://doi.org/10.1029/97jd03300>, 1997.
- 1245 Shaver, G. R., L. E. Street, Rastetter, E. B., M. T. Van Wijk, and Williams, M.: Functional
1246 Convergence in Regulation of Net CO₂ Flux in Heterogeneous Tundra Landscapes in Alaska and
1247 Sweden, *J. Ecol.*, 95, 802–817, 2007.
- 1248 Siewert, M. B., Hanisch, J., Weiss, N., Kuhry, P., Maximov, T. C., and Hugelius, G.: Comparing
1249 carbon storage of Siberian tundra and taiga permafrost ecosystems at very high spatial
1250 resolution: ECOSYSTEM CARBON IN TAIGA AND TUNDRA, *J. Geophys. Res. Biogeosci.*,
1251 120, 1973–1994, <https://doi.org/10.1002/2015jg002999>, 2015.
- 1252 Soloway, A. D., Amiro, B. D., Dunn, A. L., and Wofsy, S. C.: Carbon neutral or a sink?
1253 Uncertainty caused by gap-filling long-term flux measurements for an old-growth boreal black
1254 spruce forest, *Agric. For. Meteorol.*, 233, 110–121,
1255 <https://doi.org/10.1016/j.agrformet.2016.11.005>, 2017.
- 1256 Tarnocai, C., Canadell, J. G., Schuur, E. A. G., Kuhry, P., Mazhitova, G., and Zimov, S.: Soil
1257 organic carbon pools in the northern circumpolar permafrost region, *Global Biogeochem. Cycles*,
1258 23, 2009.
- 1259 Tramontana, G., Migliavacca, M., Jung, M., Reichstein, M., Keenan, T. F., Camps-Valls, G.,
1260 Ogee, J., Verrelst, J., and Papale, D.: Partitioning net carbon dioxide fluxes into photosynthesis
1261 and respiration using neural networks, *Glob. Chang. Biol.*, 26, 5235–5253,
1262 <https://doi.org/10.1111/gcb.15203>, 2020.
- 1263 Valentini, R.: EUROFLUX: An Integrated Network for Studying the Long-Term Responses of
1264 Biospheric Exchanges of Carbon, Water, and Energy of European Forests, in: *Fluxes of Carbon,*
1265 *Water and Energy of European Forests*, edited by: Valentini, R., Springer Berlin Heidelberg,
1266 Berlin, Heidelberg, 1–8, https://doi.org/10.1007/978-3-662-05171-9_1, 2003.
- 1267 Virkkala, A.-M., Virtanen, T., Lehtonen, A., Rinne, J., and Luoto, M.: The current state of CO₂
1268 flux chamber studies in the Arctic tundra: A review, *Progress in Physical Geography: Earth and*
1269 *Environment*, 42, 162–184, <https://doi.org/10.1177/0309133317745784>, 2018.
- 1270 Virkkala, A.-M., Abdi, A. M., Luoto, M., and Metcalfe, D. B.: Identifying multidisciplinary
1271 research gaps across Arctic terrestrial gradients, *Environ. Res. Lett.*, 14, 124061,
1272 <https://doi.org/10.1088/1748-9326/ab4291>, 2019.
- 1273 Virkkala, A.-M., Aalto, J., Rogers, B. M., Tagesson, T., Treat, C. C., Natali, S. M., Watts, J. D.,
1274 Potter, S., Lehtonen, A., Mauritz, M., Schuur, E. A. G., Kochendorfer, J., Zona, D., Oechel, W.,
1275 Kobayashi, H., Humphreys, E., Goeckede, M., Iwata, H., Lafleur, P. M., Euskirchen, E. S.,
1276 Bokhorst, S., Marushchak, M., Martikainen, P. J., Elberling, B., Voigt, C., Biasi, C., Sonnentag,
1277 O., Parmentier, F.-J. W., Ueyama, M., Celis, G., St Loius, V. L., Emmerton, C. A., Peichl, M.,
1278 Chi, J., Järveoja, J., Nilsson, M. B., Oberbauer, S. F., Torn, M. S., Park, S.-J., Dolman, H.,

- 1279 Mammarella, I., Chae, N., Poyatos, R., López-Blanco, E., Røjle Christensen, T., Jung Kwon, M.,
1280 Sachs, T., Holl, D., and Luoto, M.: Statistical upscaling of ecosystem CO₂ fluxes across the
1281 terrestrial tundra and boreal domain: regional patterns and uncertainties, *Glob. Chang. Biol.*,
1282 <https://doi.org/10.1111/gcb.15659>, 2021b.
- 1283 Virkkala, A.-M., Natali, S., Rogers, B. M., Watts, J. A., Savage, K., Connon, S. J., Mauritz, M.,
1284 Schuur, E. A. G., Peter, D., Minions, C. et al.: The ABCflux Database: Arctic-Boreal CO₂ Flux
1285 and Site Environmental Data, 1989-2020, <https://doi.org/10.3334/ORNLDAAC/1934>, 2021a.
- 1286 Voigt, C., Lamprecht, R. E., Marushchak, M. E., Lind, S. E., Novakovskiy, A., Aurela, M.,
1287 Martikainen, P. J., and Biasi, C.: Warming of subarctic tundra increases emissions of all three
1288 important greenhouse gases - carbon dioxide, methane, and nitrous oxide, *Glob. Chang. Biol.*,
1289 23, 3121–3138, <https://doi.org/10.1111/gcb.13563>, 2017.
- 1290 Wang, K., Liu, C., Zheng, X., Pihlatie, M., Li, B., Haapanala, S., Vesala, T., Liu, H., Wang, Y.,
1291 Liu, G., and Hu, F.: Comparison between eddy covariance and automatic chamber techniques for
1292 measuring net ecosystem exchange of carbon dioxide in cotton and wheat fields, *Biogeosciences*,
1293 10, 6865–6877, <https://doi.org/10.5194/bg-10-6865-2013>, 2013.
- 1294 Wang, L., Lee, X., Wang, W., Wang, X., Wei, Z., Fu, C., Gao, Y., Lu, L., Song, W., Su, P., and
1295 Lin, G.: A Meta-Analysis of Open-Path Eddy Covariance Observations of Apparent CO₂ Flux in
1296 Cold Conditions in FLUXNET, *J. Atmos. Ocean. Technol.*, 34, 2475–2487,
1297 <https://doi.org/10.1175/JTECH-D-17-0085.1>, 2017.
- 1298 Wutzler, T., Lucas-Moffat, A., Migliavacca, M., Knauer, J., Sickel, K., Šigut, L., Menzer, O.,
1299 and Reichstein, M.: Basic and extensible post-processing of eddy covariance flux data with
1300 REddyProc, *Biogeosciences*, 15, 5015–5030, <https://doi.org/10.5194/bg-15-5015-2018>, 2018.
- 1301